HEALTH EFFECTS INSTITUTE

H E I

RESEARCH REPORT No. 10

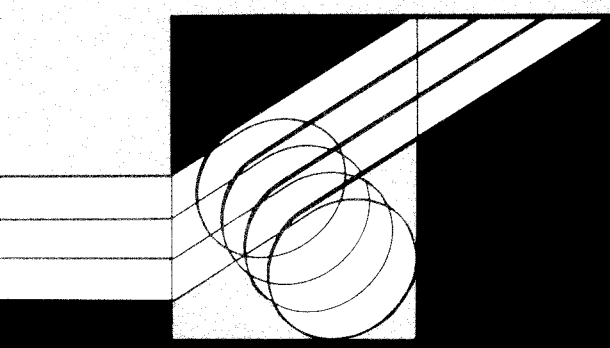

Predictive Models for Deposition of Inhaled Diesel Exhaust Particles in Humans and Laboratory Species

C.P. Yu, Ph.D., and G.B. Xu, Ph.D.

State University of New York at Buffalo
Amherst, New York

Includes the Report of the Institute's Health Review Committee

The Health Effects Institute (HEI) is a non-profit corporation founded in 1980 to assure that objective, credible, high-quality scientific studies are conducted on the potential human health effects of motor vehicle emissions.

Funded equally by the U.S. Environmental Protection Agency (EPA) and 26 automotive manufacturers or marketers in the United States, HEI is independently governed. Its research projects are selected, conducted, and evaluated according to a careful public process, including a rigorous peer review process, to assure both credibility and high scientific standards.

HEI makes no recommendations on regulatory and social policy. Its goal, as stated by former EPA Administrator William D. Ruckelshaus, is "simply to gain acceptance by all parties of the data that may be necessary for future regulations."

The Board of Directors

Archibald Cox, *Chair; Carl M. Loeb University Professor (Emeritus), Harvard Law School*
William O. Baker, *Chairman (Emeritus)* Bell Laboratories
Donald Kennedy, *President, Stanford University*
Charles W. Powers, *President, Clean Sites, Inc. and Founding Executive Director, HEI*

Officers

Thomas P. Grumbly, *Executive Director and Treasurer*
Richard M. Cooper, *Corporate Secretary*

Health Research Committee

Walter A. Rosenblith, *Chair; Institute Professor and Recent Provost, Massachusetts Institute of Technology, Foreign Secretary, National Academy of Science*
Joseph D. Brain, *Professor of Physiology, Harvard School of Public Health*
Curtis C. Harris, *Chief, Laboratory of Human Carcinogenesis, National Cancer Institute*
Barbara Hulka, *Chairperson, Department of Epidemiology, University of North Carolina*
Roger O. McClellan, *President, Inhalation Toxicology Research Institute*
Robert F. Sawyer, *Professor of Mechanical Engineering, University of California, Berkeley*
John W. Tukey, *Senior Research Statistician, and Donner Professor of Science Emeritus, Princeton University*
Mark J. Utell, *Professor of Medicine and Toxicology, University of Rochester School of Medicine*
Gerald N. Wogan, *Professor of Toxicology, Massachusetts Institute of Technology*

Health Review Committee

Robert I. Levy, *Chair; Professor of Medicine, Columbia University, Former Director, National Heart, Lung and Blood Institute*
Bernard Goldstein, *Professor and Chairman, Department of Environmental and Community Medicine, University of Medicine and Dentistry of New Jersey, Robert Wood Johnson Medical Center*
Gareth M. Green, *Professor and Chairman, Department of Environmental Science, Johns Hopkins University*
Millicent W. P. Higgins, *Associate Director for Epidemiology and Biometry, National Heart, Lung and Blood Institute*
Paul Meier, *Professor of Statistics, University of Chicago*
Sheldon D. Murphy, *Chairman, Department of Environmental Health, University of Washington*
Herbert Rosenkranz, *Professor and Chairman, Department of Environmental Health Sciences and Professor of Biochemistry, Pediatrics and Radiology, Case Western Reserve University*
Arthur Upton, *Professor and Chairman, Institute of Environmental Medicine, New York University*

Staff

Thomas P. Grumbly, *Executive Director and Treasurer*
Rashid Shaikh, *Director for Scientific Review and Evaluation*
A. Jane Warren, *Director of Research*
Judith A. Zalon, *Assistant Director for Administration*
Patrick Kinney, *Staff Scientist*
Kathleen M. Nauss, *Staff Scientist*
Harriet M. Strimpel, *Consulting Staff Scientist*
Kristine H. Templeman, *Consulting Staff Scientist*
Ann Y. Watson, *Consulting Staff Scientist*

Jessica Schwartz, *Director of Special Projects, was the production consultant for this project.*

Copyright © 1987 by Health Effects Institute

Research Agreement No. 84-5
Designed and printed by Prime Communications, Inc.

TABLE OF CONTENTS

List of Figures i

List of Tables ii

Preface — Health Effects Institute and its Research Process 1

Introduction 1

The Clean Air Act 1

Background 2

Investigators' Report — Predictive Models for Deposition of Inhaled Diesel Exhaust Particles in Humans and Laboratory Species 3

Abstract 3

Introduction 3

Specific Aims 3

Methods 4

Results 9

Summary and Conclusions 14

Acknowledgments 14

References 15

Appendix A: Mathematical Model of The Human Lung Postnatal Development 17

Introduction 17

Number of Airways and Alveoli 17

Airway Size 18

Appendix B: Lung Models for Rats, Hamsters, and Guinea Pigs 21

Health Review Committee's Report — HEI Objectives 23

Justification for the Study by HEI 23

Objectives of the Study 23

Technical Evaluation 23

Results and Interpretation 23

New Insights 24

Conclusions 24

Explanation of Some of the Technical Terms Used in This Report 25

References 26

About the Authors 27

LIST OF FIGURES

Figure 1. Total (T) and regional (head H, tracheobronchial TB, alveolar A) deposition of DEPs in human adults (age 25 or older) at mouth breathing. Conditions for calculation: (a) $\sigma_g = 4.5$, $\phi = 0.3$ and $p = 1.5$ g/cm^3, (b) lung volume (LV) = 3200 cm^3, (c) tidal volume (TV) = 500 cm^3 and respiratory frequency (RF) = 14 min^{-1}. 9

Figure 2. Total and regional deposition of DEPs in human adults at mouth breathing. Conditions for calculation: (a) MMAD = 0.2 μm, $\phi = 0.3$ and $p = 1.5$ g/cm^3, (b) LV = 3200 cm^3, and (c) TV = 500 cm^3 and RF = 14 min^{-1}. 10

Figure 3. Total and regional deposition of DEPs in human adults at different breathing modes. Conditions for calculation: (a) $\sigma_g = 4.5$, $\phi = 0.3$ and $p = 1.5$ g/cm^3, (b) LV = 3200 cm$_3$, and (c) TV = 500 cm^3 and RF = 14 min^{-1}. 10

Figure 4. Total and regional deposition of DEPs in human adults at different ventilation conditions. Conditions for calculation: (a) MMAD = 0.2 μm, $\sigma_g = 4.5$, $\phi = 0.3$ and $p = 1.5$ g/cm^3, (b) LV = 3200 cm^3, and (c) mouth breathing. 10

Figure 5. Total and regional deposition of DEPs in human adults with different lung volumes. Conditions for calculation: (a) MMAD = 0.2 μm, $\sigma_g = 4.5$, $\phi = 0.3$ and $p = 1.5$ g/cm^3, (b) TV = 500 cm^3 and RF = 14 min^{-1}, and (c) mouth breathing. 10

Figure 6. Total and regional deposition of DEPs in humans under age 25. Conditions for calculation: (a) MMAD = 0.2 μm, $\sigma_g = 1.9$, $\phi = 0.3$ and $p = 1.5$ g/cm^3, and (b) nose breathing. 12

Figure 7. Deposition distribution patterns of DEPs in humans under age 25. Conditions for calculation: (a) MMAD = 0.2 μm, $\sigma_g = 1.9$, $\phi = 0.3$ and $p = 1.5$ g/cm^3, and (b) nose breathing. 12

Figure 8. Total and alveolar deposition of DEPs in human adults and laboratory species. Conditions for calculation: (a) MMAD = 0.2 μm, $\sigma_g = 1.9$, $\phi = 0.3$ and $p = 1.5$ g/cm^3, and (b) nose breathing. 14

Figure 9. Comparison of deposition distribution patterns of DEPs between human adults and Fischer rats. Conditions for calculation: (a) MMAD = 0.2 μm, $\sigma_g = 1.9$, $\phi = 0.3$ and $p = 1.5$ g/cm^3, and (b) nose breathing. 14

Figure A-1. Total number of airways in the last three generations as a function of age. The data points are from different authors and the solid line represents Equation (A-5). 17

Figure A-2. Total number of alveoli as a function of age. The data points are from different authors and the solid line represents Equation (A-6). 17

Figure A-3. Total lung volume as a function of age. The data points are from different authors and the solid line represents Equation (A-7). 18

Figure A-4. Body height as a function of age. The data points are from different authors and the solid line represents Equation (A-11). 18

Figure A-5. Values of α_i and β_i for the ith airway generation. The data points are from Phalen et al. (1985) and the solid lines represent Equations (A-12) and (A-13). 19

Figure A-6. Alveolar diameter as a function of age. The data points are from different authors and the solid line represents the calculated result. 19

Figure B-1. Number of airways per generation for various species. 22

Figure B-2. Normalized airway diameter versus generation number for various species. 22

Figure B-3. Normalized airway cross-sectional area as a function of airway depth for various species. Dotted lines indicate the unciliated airways. 22

Figure B-4. Normalized cumulative airway volume as a function of airway depth for various species. Dotted line indicates the unciliated airways. 22

LIST OF TABLES

Table 1 Diesel Particles from a GM 5.7 Liter Engine Emission 5

Table 2 Values of d_e/d_a and $\varkappa$ for Different Values of ϕ at $\rho = 1.5$ g/cm^3 6

Table 3 Effect of Lung Model on Deposition of Diesel Exhaust Particles 11

Table 4 Effect of Nose Deposition Efficiency on Deposition of Diesel Exhaust Particles 11

Table 5 Volumetric and Surface Minute Doses in Humans Under Age 25 13

Table 6 Deposition Predictions Compared to Experimental Data on Rats 13

Table 7 Volumetric and Surface Minute Doses for Various Species 13

Table B-1 Lung Model for Rats at Total Lung Capacity 21

Table B-2 Lung Model for Hamsters at Total Lung Capacity 21

Table B-3 Lung Model for Guinea Pigs at Total Lung Capacity 21

PREFACE

HEALTH EFFECTS INSTITUTE AND ITS RESEARCH PROCESS

The Health Effects Institute (HEI) is an independent nonprofit corporation which, according to its charter, is "organized and operated...specifically to conduct or support the conduct of, and to evaluate, research and testing relating to, the health effects of emissions from motor vehicles".

It is organized in the following ways to pursue this purpose:

INDEPENDENCE IN GOVERNANCE

HEI is governed by a four-member Board of Directors whose members are William O. Baker, Chairman Emeritus of Bell Laboratories and Chairman of the Board of Rockefeller University; Archibald Cox, Carl M. Loeb University Professor (Emeritus) at Harvard University; Donald Kennedy, President of Stanford University; and Charles Powers, President, Clean Sites, Incorporated. Professor Cox chairs the Board. These individuals, who select their own successors, were chosen initially, after consultation with industry and other individuals, by then Environmental Protection Agency Administrator Douglas M. Costle.

TWO-SECTOR FINANCIAL SUPPORT

The Institute receives half of its funds from the United States government through the Environmental Protection Agency and half from the automotive industry. Twenty-six leading manufacturers of vehicles or engines that are certified for use on U.S. highways contribute to the Institute's budget, in shares proportionate to the number of vehicles or engines that they sell.

RESEARCH PLANNING AND PROJECT EVALUATION

HEI is structured to define, select, support, and review research that is aimed at investigating the possible health effects of mobile source emissions. Its research program is devised by the Health Research Committee, a multidisciplinary group of scientists knowledgeable about the complex problems involved in determining the health effects of mobile source emissions. The Committee seeks advice from HEI's sponsors and from other sources prior to independently determining the research priorities of the Institute.

After the Health Research Committee has defined an area of inquiry, the Institute announces to the scientific community that research proposals are being solicited on a specific topic. Applications are reviewed first for scientific quality by an appropriate expert panel. Then they are reviewed by the Health Research Committee both for quality and for relevance to the mission-oriented research program. Studies recommended by the Committee undergo final evaluation by the Board of Directors, which also reviews the procedures, independence, and quality of the selection process.

When a study is completed, a draft final report is reviewed by a separate HEI committee, the Health Review Committee. Members are expert scientists representing a broad range of experience in environmental health sciences. The Health Review Committee has no role either in the review of applications or in the selection of projects and investigators for funding. This Committee assesses the scientific quality of each study and evaluates its contribution to unresolved scientific questions.

Each funded proposal is assigned in advance of completion to a member of the Health Review Committee, who acts as "primary reviewer". When the draft report is received, the primary reviewer directs a peer review by technical experts and, when appropriate, by a biostatistician. After the investigator has had a chance to comment on the technical evaluations, the primary reviewer drafts a review. This document is sent to the investigator for comment. It is subsequently examined by the full Health Review Committee and revised as necessary. The investigator's final report, as well as the Health Review Committee's report, are then made available to the sponsors and to the public after evaluation by the HEI Board of Directors.

All HEI investigators are urged to publish the results of their work in the peer-reviewed literature. The timing and nature of HEI report releases are tailored to ensure that the Health Review Committee's report does not interfere with the journal publication process. The report of the Health Review Committee will be as thorough as necessary to evaluate any individual report.

INTRODUCTION

A Request for Applications (RFA 83-3) solicitating proposals on the "Dose of Airborne Pollutants to Target Tissues" was issued by the HEI in the summer of 1983. Dr. C.P. Yu of the State University of New York at Buffalo submitted a proposal entitled, "Determination of Lung Doses of Diesel Exhaust Particulates" (later retitled "Predictive Models for Deposition of Inhaled Diesel Exhaust Particles in Humans and Laboratory Species"). The HEI approved the two-year project and authorized a total expenditure of $149,030. The project began in July, 1984, and the final report was accepted by the Health Review Committee in January, 1987. The Health Review Committee's report, which follows the investigators' report, is intended to place the investigators' final report in perspective as an aid to the sponsors of the HEI and to the public.

THE CLEAN AIR ACT

The Environmental Protection Agency (EPA) sets standards for diesel (and other) emissions under Section 202 of the Clean Air Act, as amended in 1977. Section 202(a)(1) directs the Administrator to "prescribe (and from time to time revise)... standards applicable to the emission of any air pollutant from any class or classes of new motor vehicles or new motor vehicle engines, which in his judgment cause, or contribute to, air pollution which may reasonably be anticipated to endanger

public health or welfare." Section 202(a)(3)(A)(i) specifically directs the Administrator to "prescribe regulations... applicable to emissions of carbon monoxide, hydrocarbons, and oxides of nitrogen from classes...of heavy-duty vehicles or engines..." Section 202(a)(3)(A)(iii) similarly requires regulations applicable to emissions of particulate matter from classes or categories of vehicles.

Under these provisions, the EPA has taken regulatory actions with respect to diesel engines. In 1980, the Agency set light duty diesel particulate standards, and, in 1984, granted a two- year delay in their effective date. In addition, the Agency established emissions averaging in 1983, and it set nitrogen oxides standards in 1985. For heavy duty diesel engines, the Agency set hydrocarbon and carbon monoxide standards in 1983, and nitrogen oxides and particulate standards in 1985. Research on the deposition of diesel exhaust particulate in the respiratory tract of humans and other species, as well as the development of a mathematical model to predict such deposition, can contribute knowledge useful for making the risk assessments on which emissions standards are based in part.

BACKGROUND

The overall assessment of the health effects from exposure to diesel exhaust involves a synthesis of numerous complex variables, such as extent of exposure, target tissue dose, toxicity of the original and metabolized agent(s), and variations in host susceptibility due to genetic predisposition, age, gender, pre-existing disease, and concomitant exposures. The health effects of diesel emissions are of concern for several reasons, including the small size of the particulate which allows entry into the respiratory tract, the genotoxicity of a number of chemicals associated with the particulate, and the recently reported carcinogenicity of whole diesel exhaust in animal studies (Ishinishi et al., 1986)§. Therefore, determination of the dose of diesel particulate material to pulmonary tissues is important for relating ambient exposures to potential human health effects.

At the present time, no direct method exists for experimentally measuring the dose of diesel exhaust particulate to the cells and tissues of the respiratory tract. However, tissue doses can be estimated by determining the amount of particulate retained in the respiratory tract at any time; retention represents the balance of the two processes, deposition and clearance. Initial deposition sites of inhaled particulate influence clearance rates because various regions of the respiratory tract clear deposited material at different rates. For example, material deposited in the nose, trachea, or airways lined with ciliated cells are cleared more rapidly than material deposited distally in unciliated regions. Therefore, better quantification of retention, or estimated tissue dose, can be achieved with improved characterization of regional deposition patterns.

Numerous techniques to measure aerosol deposition are currently available (Valberg, 1985)§. Their use in humans, however, is limited because of their degree of invasiveness, lack of specificity, or expense. Mathematical approaches can be used to model the behavior of particles in the respiratory tract; such models can guide experimental studies and supplement empirical observations.

Airborne particles are removed from inhaled air because of their sedimentation, impaction, diffusion, or inception onto lung surfaces (reviewed by Schlesinger, 1987)§. The effectiveness of these mechanisms depends on three key parameters: particle properties, airway geometry, and breathing pattern. The definition of each of these parameters presents difficulties. Particle properties can be measured, but they may change in unpredictable ways in the high-humidity environment of the respiratory tract. Among the various characteristics of particles, their size is the most important determinant of regional deposition. Particle diameter and diameter distribution data are critical to deposition model development. These characteristics of particles can usually be measured experimentally.

Characterization of airway geometry is a more difficult task. The anatomy of the respiratory tract is not well described in humans, and it changes dramatically from the point of inhalation to the terminal airspaces. Branching patterns, airway diameter, and conducting airway length exhibit considerable inter- and intraspecies variability. The lack of an extensive morphometric data base has led to the adoption of simplified anatomical descriptions in deposition models.

Finally, the ventilatory pattern (e.g., breathing frequency, volume of inhaled air per breath) and mode of inhalation (e.g., nasal, oronasal) influence the deposition pattern of inhaled particles. However, the aerodynamics of respiration is frequently measured only at the mouth; flow profiles, asymmetry of filling, and turbulence within the lung are less well known. In addition, flow profiles change between inspiration and expiration. Because of the difficulties discussed above, the formulation of predictive deposition models presents a formidable challenge. Such modeling involves making simplifying assumptions as well as dealing with the input variables one at a time, rather than in combination which would be more realistic.

Ideally, a mathematical model should incorporate realistic descriptions of particle properties, airway geometry, and breathing patterns, so that useful predictions of regional deposition can be made. By varying the input values for these parameters, the model can be applied to real-life problems. The "consumer" of a theoretical model would like to relate atmospheric concentrations of airborne particulate to certain biological outcomes in the whole spectrum of the human population — the young, the physically active adult, the elderly, and the diseased. Each of these subpopulations differs in lung anatomy and in ventilation from normal, resting adults; this ultimately affects the amount and location of deposited particles in the lung.

The goals of the study by Dr. C.P. Yu were: to develop a mathematical model that considers the physical characteristics of diesel particulate, and that predicts the dynamics of diesel particulate deposition in the respiratory tract; to elaborate the model to include the age range of humans from infancy to adulthood; and to validate the model against experimental measurements in laboratory animals.

§ See References on page 26.

INVESTIGATORS' REPORT

by C. P. Yu, Ph.D., and G. B. Xu, Ph.D.

Predictive Models for Deposition of Inhaled Diesel Exhaust Particles in Humans and Laboratory Species

ABSTRACT

Mathematical and computer models of the respiratory tracts of human beings and of laboratory animals (rats, hamsters, guinea pigs) were used to estimate the deposition patterns of inhaled diesel exhaust particles from automobile emissions. The accuracy of these models was tested by comparing the calculated depositions in laboratory animals with actual laboratory data. Our goal was to be able to predict the relation between exposure to diesel exhaust particles and the deposition of these particles in the lungs of humans of various ages.

Diesel exhaust particles are aggregates with a mass median aerodynamic diameter of approximately 0.2 μm. Their actual size depends on the conditions under which they are generated. Using an appropriate particle model, we derived mathematical expressions that describe the effects of diffusion, sedimentation, impaction, and interception on the deposition of these particles. Because of their small size, we found that most diesel exhaust particles deposited through diffusion, and that the role of the other mechanisms was minor.

Anatomical models of the human lung from birth to adulthood, as well as models of the lungs of laboratory species were formulated mathematically using available morphometric data. We used these lung models, together with the corresponding ventilation conditions of each species, to calculate deposition of diesel exhaust particles in the lungs. Under normal breathing conditions, we calculated that 7 to 13 percent (depending on particle size) of inhaled diesel exhaust particles deposit in the alveolar region of the adult human lung. Although the breathing mode (nose or mouth breathing) did not appear to affect alveolar deposition, increasing the minute ventilation (the number of breaths per minute multiplied by the tidal volume) increased alveolar deposition significantly.

The calculated deposition patterns for diesel exhaust particles in younger humans (under age 25) were similar. However, with the exception of alveolar deposition in very young children (under age two), predicted deposition was greater in the lungs of younger humans than in the lungs of humans age 25 or older. For an equal exposure, the surface minute dose (particle mass deposited per minute per unit surface area) of unciliated airways appeared to change profoundly with age. Predicted dose was maximal in the lung models of two-year-old children. At this age, the calculated dose was approximately twice as high as in the mature adult lung.

Deposition predictions for laboratory species compared favorably with existing data. Distribution of deposition was found to be similar among all species studied, although surface minute dose decreased with body weight.

INTRODUCTION

Although diesel engine cars provide about 25 percent higher fuel economy and reduce the exhaust emissions of carbon monoxide and hydrocarbons as compared to an equal-performance car with a conventional gasoline engine, they produce significantly more particulate matter. These particles consist principally of combustion-generated carbonaceous soot, on which variable amounts of potentially toxic, solvent-extractable organic materials are adsorbed. Because these particles are submicron in size, they can penetrate and deposit in the alveolar region of the lung.

The health effects of diesel emissions have been the subject of investigation for many years, but the results are not conclusive. For example, it was reported (Barth and Blacker, 1978) that diesel exhaust had a mutagenic effect in bacterial assays, which indicated that such inhaled particles might be carcinogenic. However, epidemiological studies, such as those conducted by the British Medical Research Council on London bus workers between 1955 and 1974 (Waller, 1980), and some recent inhalation studies on animals (Gross, 1981; Chan et al., 1981; Lee et al., 1983), claimed that the airborne diesel particles posed no serious threat to public health. These contradictions have yet to be explained, but may possibly be the result of the differences in conditions and experimental methods employed among all of these studies. Chan et al. (1984) recently found that diesel particles accumulated gradually in the lungs of rats in high and median exposure concentration groups, but not in the low exposure group. The incidence of lung tumors also increased in rats that were exposed to high levels of diesel particles for prolonged periods (Heinrich et al., 1985; Mauderly et al., 1985). These findings suggested that the long-term lung burden, and hence the potential hazardous effect of diesel particles, was closely associated with the exposure concentration and its temporal variation.

SPECIFIC AIMS

This project was designed to characterize the deposition pattern of diesel exhaust particles (DEPs) in the respiratory tract of humans and laboratory species (rats, hamsters, guinea pigs). Our goal was to be able to predict the relation between exposure to diesel particles and the deposition of these particles in the lungs of humans of various ages, on the basis of

mathematical models. Specifically, we wished to provide information on:

- The deposition pattern of inhaled DEPs in healthy human adults (age 25 or older) under normal breathing conditions.
- The effect of the ventilation state on deposition pattern.
- The deposition pattern for younger humans.
- The deposition pattern in laboratory species and its relationship to humans.

Particular attention was given to the deposition fraction of DEPs in the alveolar region of the lung, where particles are retained for long time periods.

METHODS

Deposition of aerosol particles in the respiratory tract is determined by three major factors: the physical and aerodynamic characteristics of the particles; the architecture of the respiratory tract; and the ventilation conditions. Data for these factors, which are available in the literature, were extensively reviewed and formulated in mathematical expressions. Models of deposition were then developed and used to predict deposition. Predicted deposition for rats was validated with existing experimental data.

GENERAL CONSIDERATION ON DEPOSITION MODELING

Based upon differences in physiological functions and particle clearance characteristics, the respiratory tract is often subdivided into the naso- or oro-pharyngeal region, tracheobronchial region, and alveolar region (Task Group on Lung Dynamics, 1966). The deposition of inhaled particles in the respiratory tract is normally considered at the regional level. The naso- or oro-pharyngeal region extends from the anterior nares or lips to the larynx. The tracheobronchial region covers the airways from the trachea to terminal bronchioles inclusive. Beginning with the posterior portions of the nares, the nasal turbinates, the trachea and bronchial airways are ciliated and lined by mucus arising from glands and secretory cells. The airways beyond the terminal bronchioles are the alveolar region of the lungs, where gas exchange takes place. These airways are nonciliated and are lined with surfactants.

Because of the presence of many repeating bifurcating airways, air flow patterns in the respiratory tract are very complex. In humans for example, the Reynolds number of the flow decreases from a few thousand in the trachea to a few hundredths in the alveolar duct. This corresponds to a transition from turbulent flow to Stokes flow. In developing a particle deposition model, it is necessary to simplify the airway structure by using idealized models and to assume idealized flow patterns in the model airways.

There are four mechanisms which cause deposition of diesel particles within the respiratory tract: impaction, sedimentation, interception, and diffusion. The contribution from each individual mechanism to deposition, however, depends upon the particle size and flow rate.

Under normal breathing conditions, inertial impaction is most important for large particles which have aerodynamic diameters (diameters of a unit-density sphere that has the same terminal velocity as the given particle) greater than a few microns. The major deposition sites are the nasal and oral air passages and the tracheobronchial airways. Since impaction deposition occurs instantaneously, its efficiency is highly sensitive to the local airway geometry and flow pattern. As a result, large intersubject variability is often observed if deposition is governed by this mechanism.

Particle deposition by sedimentation, on the other hand, is a time-dependent process. Consequently, deposition by this mechanism increases with particle residence time in the airways. For particles with aerodynamic diameters from 0.5 to 2 μm, deposition is predominated by sedimentation in the small airways.

Particle deposition by interception occurs when particles come in contact with the carina of an airway bifurcation. Because the particle size is very small compared to the airway dimension, interception is normally insignificant except for large particles in the small airways.

Particle diffusion is caused by its collision with the air molecules. The rate of diffusion increases with decreasing geometrical diameter of the particle. Similar to sedimentation, deposition by diffusion increases with particle residence time in the airway. For particle diameters smaller than 0.5 μm, diffusion plays a major role in deposition.

The understanding of various deposition mechanisms and the contribution to deposition from each individual mechanism for different particle size ranges is essential to arriving at proper formulae for deposition calculation.

PARTICLE MODEL

Previous studies (Kittelson and Dolan, 1980; Soderholm, 1981) have shown that DEPs are aggregates formed from primary spherical particles that are 15-30 nm in diameter. Aggregates of these particles are irregularly shaped and range in size from a few molecular diameters to tens of microns. The size distribution of the aggregates, however, depends upon engine design, fuels used, engine operating conditions, and thermodynamic conditions in the exhaust air.

Because the size of these aggregated particles varies so markedly, sampling the entire spectrum of DEPs with a single type of instrument would be impossible. Cheng et al. (1984) summarized the results of various investigators who measured diesel engine emissions in different environments using different measuring devices. When diesel particles were sampled in tunnels in which they were diluted by air before entering the exposure chambers, their mass median aerodynamic diameter (MMAD) ranged from 0.19 to 0.54 μm. The size distribution was found to be approximately lognormal, with

a geometric standard deviation σ_g greater than 4. However, Chan et al. (1981; 1984), who measured diesel particles using a quick dilution method, reported a smaller MMAD (0.1-0.15 μm) and a much smaller value of σ_g (1.9). In the actual roadway environment, diesel exhaust particles would, because of the short residence time (less than 1 sec) and high dilution ratio (greater than 1000:1), most likely have a smaller MMAD and σ_g than those particles measured in the laboratory. The density of diesel exhaust particles has not been adequately investigated, but the best estimate to date, made by Soderholm (1981), is about 1.5 g/cm^3. Table 1 summarizes the size distribution of diesel particles reported by various investigators.

Deposition behavior of irregularly shaped particles, such as DEPs, in model airways is not well understood. Neither experimental nor theoretical results are available at this time, although such information is important to the formulation of a lung deposition model. In this study, we used the equivalent spherical particle model described below to derive mathematical expressions for the effects of impaction, sedimentation, interception, and diffusion on deposition efficiency in an airway.

We considered each diesel particle to be a cluster-shaped aggregate consisting of solid primary particles with a bulk density p within a spherical envelope of diameter d_e. The ratio of the space actually occupied by solid particles in the envelope to the overall envelope volume would then be the packing density, ϕ, which determines the dynamic shape factor, $\varkappa$, of the particle (Kasper, 1982). Since the air density is negligibly small compared to p, the effective density of the spherical envelope, p_e, is:

$$p_e = p\left(\frac{d_v}{d_e}\right)^3 = p\phi, \qquad (1)$$

where d_v is the volume equivalent diameter of the diesel particle.

By definition, the aerodynamic diameter of a particle is given by:

$$d_a = d_e\left(\frac{C_e}{C_a}\right)^{1/2}\left(\frac{p_e}{p_o}\right)^{1/2}, \qquad (2)$$

where $p_o = 1$ g/cm^3, C_e and C_a are, respectively, slip coefficients associated with diameters d_e and d_a, and C_x is given by the expression (Davies, 1945):

$$C_x = 1 + \frac{2\lambda}{d_x}\left[1.257 + 0.4\exp\left(-\frac{0.55 d_x}{\lambda}\right)\right], \qquad (3)$$

in which λ is the mean free path of air molecules.

Combining Equations (1) and (2), we get:

$$\frac{d_e}{d_a} = \phi^{-1/2}\left(\frac{C_a}{C_e}\right)^{1/2}\left(\frac{p}{p_o}\right)^{1/2}. \qquad (4)$$

Since d_e determines the mechanical mobility of the particle, the dynamic shape factor, $\varkappa$, can be written as (Kasper, 1982):

$$\varkappa = \frac{d_e C_v}{d_v C_e} = \phi^{-1/3}\left(\frac{C_v}{C_e}\right). \qquad (5)$$

Equations (4) and (5), together with Equation (3), determine the values of d_e/d_a and $\varkappa$ for a given p and ϕ. Table 2 shows these results for different values of ϕ and a constant value of $p = 1.5$ g/cm^3. As ϕ increases, both d_e/d_a and $\varkappa$ decrease, and when $\phi = 1$, they reach respective values of 0.75 and 1, which is the case for a solid sphere.

Table 1. Diesel Particles from a GM 5.7 Liter Engine Emission

Driving Pattern	Sampling Environment	Measuring Devices	Size (μm)	σ_g	Investigators
16 kmph	Roadway	Optical Counter/EAA[a]	0.22 VMD[c]	—	Dolan and Kittelson (1979)
80 kmph	Roadway	Optical Counter/EAA	0.31 VMD	—	Dolan and Kittelson (1979)
65 kmph	Exposure Chamber	Impactor	0.17-0.19 MMAD[d]	1.8 ~ 1.9	Chan et al. (1981) Soderholm (1981)
56 kmph with load	Dilution Tunnel	Impactor/EAA	0.46 MMAD	—	McCain and Drehmel (1981)
56 kmph without load	Dilution Tunnel	Impactor/EAA	0.33 MMAD	—	McCain and Drehmel (1981)
Federal Test Procedure	Dilution Tunnel	Impactor/PFDB[b]	0.23-0.26 MMAD	~ 4.5	Cheng et al. (1984)

(a) Electrical aerosol analyzer. (b) Parallel flow diffusion battery.
(c) Volume median diameter. (d) Mass median aerodynamic diameter.

Table 2. Values of d_e/d_a and $\varkappa$ for Different Values of ϕ at $p = 1.5$ g/cm^3

ϕ	d_e/d_a	$\varkappa$
0.2	1.63	1.778
0.3	1.35	1.553
0.4	1.20	1.411
0.5	1.10	1.310
1.0	0.75	1.000

As shown in Table 1, impactors are often used to determine the size of DEPs and the results are expressed in terms of aerodynamic diameter. For this reason, it is convenient to consider the diesel particle as equivalent to a polydisperse aerosol with the measured values of MMAD and σ_g. For each particle with aerodynamic diameter d_a, there is a corresponding envelope diameter d_e from Equation (4). While impaction and sedimentation are governed by d_a, diffusion and interception are controlled by d_e according to the particle model we proposed. In view of the measured particle size distribution, diffusion is probably the predominant deposition mechanism for diesel particles. However, large particles, although they constitute a small count percentage of all particles in diesel exhaust, may also contribute to deposition by impaction, sedimentation, and interception.

LUNG ARCHITECTURE

Lung architecture affects particle deposition in several ways: the linear dimension of the airway is related to the distance the particle travels before it contacts the airway surface; the air flow velocity by which the particles are transported is determined by the cross-section of the airway for a given volumetric flowrate; and flow characteristics in the airways are influenced by the airway diameter and branching patterns. Thus theoretical prediction of particle deposition depends, to a large extent, on the lung model chosen.

LUNG MODELS FOR MATURE ADULTS (AGE 25 OR OLDER)

Several existing models for mature human lungs exist. The widely used and simplest model among them is the symmetric lung model by Weibel (1963). In Weibel's model, the airways are assumed to be a dichotomous branching system with 24 generations. Beginning with the 18th generation, increasing numbers of alveoli are present on the wall of the airways and the last three generations are completely alveolated. Thus, the alveolar region in this model consists of all the airways in the last seven generations. In this study, Weibel's model was again used as the principal lung model for deposition calculation. However, calculations also were made with the lung models of Olson et al. (1970), Hansen and Ampaya (1975), and Yeh and Schum (1980), for the purposes of comparison, because differences in deposition using different lung models may represent intersubject variability within a population (Yu and Diu, 1982).

Olson's model is distinguished by the asymmetric branching of airways. This model has considerably fewer numbers of airways. The model of Hansen and Ampaya is symmetric. It has a greater respiratory bronchiolar and ductual cross-sectional area, and a greater alveolar surface area, but has fewer airway structures than does Weibel's model. The lung model of Yeh and Schum is structurally identical to Weibel's model but the airways are larger and shorter. In addition, Yeh's model specifies the branching angle of the bifurcation and the angle of inclination of the airway with gravity. Different lung models have been compared in detail elsewhere (Yu and Diu, 1982).

LUNG MODELS FOR CHILDREN AND ADULTS UNDER AGE 25

An immature lung is not simply a proportionately smaller version of the adult lung. After birth each structural component of the lungs—airways, alveoli, and blood vessels—develops and grows at a different rate. To estimate the deposition pattern of diesel particles in children, it was necessary to first understand how these structures grow. Therefore, we developed a mathematical model of lung growth from birth to adulthood (age 25) on the basis of available morphometric measurements. Since the morphometric data were not complete, data were extrapolated whenever necessary.

Our mathematical model reflects two principal characteristics of human lung development (Reid, 1977): (1) the bronchial tree is fully developed at birth but the airway size increases with age, and (2) the pulmonary airways and alveoli continue to develop after birth, increasing in number until eight years of age, and increasing in size until the chest wall is fully grown. The model also assumes a lung structure with dichotomous branching of airways and it matches Weibel's model A when evaluated at the age of 25 years, the age at which the lung is considered to be mature. A complete description of the model can be found in Appendix A.

Information on the development of airway size in the head region during postnatal growth is scarce. From the available measurements of the distance from the nasion to the anterior nasal spine in humans from the ages of 4 to 15 years (Boersma et al., 1979), this distance appears to grow at a rate similar to that of the tracheal diameter. In calculating deposition efficiency in the head, it was therefore assumed that during postnatal life, all airway dimensions in the head region are proportional to the tracheal diameter.

LUNG MODELS OF LABORATORY SPECIES

The deposition of diesel particles was also studied in three common laboratory species: rats, hamsters, and guinea pigs. The lung models for rats and hamsters were reported by Schum

and Yeh (1980) and for guinea pigs by Schreider and Hutchens (1979) on the basis of cast measurements. Perhaps because of the difference in measurement techniques, there are significantly fewer airway bifurcations or generations in the guinea pig model than in other animal models.

Appendix B presents the lung model data for various species and compares them with Weibel's model for humans. The airway dimensions given in Tables B-1 to B-3 were measured at the total lung capacity. For a normal lung volume, which is about 40 percent of the total lung capacity (Stahl, 1967), these dimensions have to be scaled down. It was assumed that any linear dimension of the lung was proportional to the cubic root of the lung volume. For members of the same species with different body weights, we also assumed that the total lung capacity was proportional to the body weight.

DEPOSITION IN THE HEAD REGION

Particle deposition in the naso- or oro-pharyngeal region is referred to as head or extrathoracic deposition. The amount of particles that enters the lung depends upon the breathing mode. Normally, more particles are collected via the nasal route than in the oral route because of the nasal hairs and the more complex air passages of the nose. Since the residence time of diesel particles in the head region during inhalation is very small (about 0.1 sec for human adults at normal breathing), diffusional deposition is insignificant and the major deposition mechanism is impaction. The following empirical formulas derived by Yu et al. (1981) for human adults were adopted for this study. These formulas were derived from a comprehensive analysis of pertinent experimental data reported in the literature for particles with aerodynamic diameters ranging from 0.2 to 23 μm.

For mouth breathing:

$$H_{in} = 0,\ \sigma_{in} = 0; \qquad \text{for } d_a^2Q \le 3000 \qquad (6)$$

$$H_{in} = -1.117 + 0.324 \log(d_a^2Q),\ \sigma_{in} = 0.144; \qquad \text{for } d_a^2Q > 3000 \qquad (7)$$

$$H_{ex} = 0,\ \sigma_{ex} = 0; \qquad (8)$$

and for nose breathing:

$$H_{in} = -0.014 + 0.023 \log(d_a^2Q),\ \sigma_{in} = 0.034; \qquad \text{for } d_a^2Q \le 337 \qquad (9)$$

$$H_{in} = -0.959 + 0.397 \log(d_a^2Q),\ \sigma_{in} = 0.145; \qquad \text{for } d_a^2Q > 337 \qquad (10)$$

$$H_{ex} = 0.003 + 0.033 \log(d_a^2Q),\ \sigma_{ex} = 0.046; \qquad \text{for } d_a^2Q \le 215 \qquad (11)$$

$$H_{ex} = -0.851 + 0.399 \log(d_a^2Q),\ \sigma_{ex} = 0.140; \qquad \text{for } d_a^2Q > 215 \qquad (12)$$

where H is the mean deposition efficiency in the head, σ is the standard deviation, the subscripts in and ex denote inspiration and expiration, respectively, d_a is the particle aerodynamic diameter in μm, and Q is the air flowrate in cm^3/sec.

Formulas to calculate deposition of diesel particles in the head region of children were derived from those for adults using the theory of similarity, which assumes that the air passage in the head region is geometrically similar for all ages, and that the deposition process is characterized by the Stokes number of the particle. Thus, the set of empirical equations from (6) through (12) were transformed into the following form:

For mouth breathing:

$$H_{in} = 0, \qquad \text{for } d_a^2Q \le 3000 \qquad (13)$$

$$H_{in} = -1.117 + 0.972 \log K + 0.324 \log(d_a^2Q), \qquad \text{for } d_a^2Q > 3000 \qquad (14)$$

$$H_{ex} = 0, \qquad (15)$$

and for nose breathing:

$$H_{in} = -0.014 + 0.690 \log K + 0.023 \log(d_a^2Q), \qquad \text{for } d_a^2Q \le 337 \qquad (16)$$

$$H_{in} = -0.959 + 1.191 \log K + 0.397 \log(d_a^2Q), \qquad \text{for } d_a^2Q > 337 \qquad (17)$$

$$H_{ex} = 0.003 + 0.099 \log K + 0.033 \log(d_a^2Q), \qquad \text{for } d_a^2Q \le 215 \qquad (18)$$

$$H_{ex} = -0.851 + 1.197 \log K + 0.399 \log(d_a^2Q), \qquad \text{for } d_a^2Q > 215 \qquad (19)$$

where K is the ratio of the linear dimension of the air passages in the head region of adults to that of children, which was assumed to be the same as the ratio of adult/child tracheal diameters.

For laboratory animals, no formulas are available in the literature that predict deposition in the head region. Experimental data of deposition in this region are also limited to a few studies. Raabe et al. (1977) measured the deposition of spherical aluminosilicate particles in the nose region of rats and hamsters. Similar measurement using spherical unit-density particles was made by Schreider and Hutchens (1979) for guinea pigs. On the basis of these data, the following empirical equations were derived for deposition prediction of diesel particles in the nose of animal species.

For rats:

$$H_{in} = H_{ex} = 0.046 + 0.009 \log(d_a^2Q), \qquad \text{for } d_a^2Q \le 13.33 \qquad (20)$$

$$H_{in} = H_{ex} = -0.522 + 0.514 \log(d_a^2Q), \qquad \text{for } d_a^2Q > 13.33 \qquad (21)$$

for hamsters:

$$H_{in} = H_{ex} = 0.048 + 0.008 \log(d_a^2Q), \qquad \text{for } d_a^2Q \le 2.13 \qquad (22)$$

$$H_{in} = H_{ex} = -0.089 + 0.423 \log(d_a^2Q), \qquad \text{for } d_a^2Q > 2.13 \qquad (23)$$

and for guinea pigs:

$$H_{in} = H_{ex} = 0.027 + 0.009 \log(d_a^2Q), \qquad \text{for } d_a^2Q \le 35.6 \qquad (24)$$

$$H_{in} = H_{ex} = -0.789 + 0.535 \log(d_a^2Q), \qquad \text{for } d_a^2Q > 35.6 \qquad (25)$$

LUNG DEPOSITION MODEL

Inhaled diesel particles which escape capture in the head during inspiration will enter the trachea and subsequently the bronchial airways and alveolar spaces. Several theoretical deposition models for monodisperse spherical particles in these regions of the respiratory tract have been proposed in the past and the subject was recently reviewed by Morrow and Yu (1985). Specifically, there are three major elements in constructing a theoretical deposition model. First, an anatomical model of airways simulating the real structure must be

specified. Secondly, deposition efficiency in each airway due to various deposition mechanisms must be derived. Finally, a computational procedure must be developed to account for the transport and deposition of the particles in the airways.

The deposition model adopted in this study is the one previously developed by Yu and Diu for monodisperse spherical aerosols (1983). This model has given excellent agreement with experimental data on human adults over a wide range of ventilation conditions and particle sizes including submicronic particles. Since DEPs are polydisperse, deposition calculation was carried out by superimposing the deposition results of many monodisperse aerosols, each with different diameter and concentration (Diu and Yu, 1983).

In the deposition model of Yu and Diu, the branching airways are viewed as a chamber model shaped like a trumpet. The cross-sectional area of the chamber varies with airway depth, x, measured from the beginning of the trachea. At the last portion of the trumpet, additional cross-sectional area is present to account for the alveolar volume per unit length of the airways.

Assuming that the airways expand and contract uniformly during breathing, the equation for the conservation of particles takes the form:

$$\beta (A_1 + A_2) \frac{\partial c}{\partial t} + Q \frac{\partial c}{\partial x} = - Qc\eta \qquad (26)$$

where c is the mean particle concentration at a given x and time t; A_1 and A_2 are, respectively, the summed cross-sectional area (or volume per unit length) of the airways and alveoli at rest; η is the particle uptake efficiency per unit length of the airway surface; β is an expansion factor, given by

$$\beta = 1 + \frac{V_t}{V_\ell} \qquad (27)$$

and Q is the air flow rate, varying with x and t according to the relation

$$\frac{Q}{Q_o} = 1 - \frac{V_x}{V_\ell} \qquad (28)$$

In Equations (27) and (28), V_t is the volume of new air in the lungs and V_x and V_ℓ are, respectively, the accumulated airway volume from x = 0 to x, and total airway volume at rest.

Equation (26) can be solved using the method of characteristics with appropriate initial and boundary conditions; the amount of particle deposited between location x_1 and x_2 from time t_1 to t_2 can then be found from the expression

$$DE = \int_{t_1}^{t_2} \int_{x_1}^{x_2} Qc\eta dxdt \qquad (29)$$

For diesel particles, η is the sum of those due to the individual deposition mechanisms described above, i.e.,

$$\eta = \eta_I + \eta_S + \eta_P + \eta_D \qquad (30)$$

where η_I, η_S, η_P and η_D are, respectively, the deposition efficiencies per unit length of the airway due to impaction, sedimentation, interception, and diffusion. On the basis of the particle model described above, we obtained the expressions for η_I, η_S, η_P, and η_D in the following form:

$$\eta_I = \frac{0.768}{L} (St)\Theta, \qquad (31)$$

$$\eta_S = \frac{2}{\pi L} \left[2\epsilon \sqrt{1-\epsilon^{2/3}} - \epsilon^{1/3} \sqrt{1-\epsilon^{2/3}} + \sin^{-1}\epsilon^{1/3} \right] \qquad (32)$$

$$\eta_P = \frac{4}{3\pi L} (\Gamma - \frac{\Gamma^3}{32}) \qquad (33)$$

and

$$\eta_D = \frac{1}{L} \left[1 - 0.819 \exp(-14.63\Delta) - 0.0976 \exp(-89.22\Delta) - 0.0325 \exp(-228\Delta) - 0.0509 \exp(-125\Delta^{2/3}) \right] \qquad (34)$$

for Reynolds number of the flow smaller than 2000, and

$$\eta_D = \frac{4}{L} \Delta^{1/2} (1 - 0.444\Delta^{1/2}) \qquad (35)$$

for Reynolds number greater than or equal to 2000. $St = d_a^2 u/(18\mu R)$ is the particle Stokes number,

$$\Theta = L/(8R)$$

$$\epsilon = 3\mu u_S L/(32uR)$$

$$\Gamma = d_e/R$$

and $$\Delta = DL/(4R^2 u)$$

in which u is the air velocity in the airway; μ is the air viscosity; L and R are, respectively, the length and radius of the airway; $u_S = C_a d_a^2/(18\mu)$ is the particle settling velocity and $D = C_e kT(3\pi\mu d_e)$ is the diffusion coefficient with k denoting the Boltzmann constant and T the absolute temperature.

The expressions for η_S and η_D were derived for a Poiseulle flow (Pich, 1972; Harris and Fraser, 1976) because the deposition of diesel particles by these mechanisms takes place mainly in the small airways in which the velocity profile is parabolic. For η_D, we used both expression (34), which was derived for the parabolic flow (Ingham, 1975), and expression (35), derived for the slug flow (Landhal, 1963). The latter formula accounted, to some extent, for the effect of the velocity profile on the collection efficiency of the particles in major airways. The expression for η_I was derived from a bend model (Chan and Yu, 1982). This formula showed good agreement with the experimental data of impaction deposition from a lung cast consisting of five generations of bifurcating airways. In the deposition model, we also assumed that $\eta_I = \eta_P = 0$ for expiration, while η_D and η_S had the same expressions for both inspiration and expiration.

During the pause, only diffusion and sedimentation are present. We assumed that the combined deposition efficiency in an airway, E, is equal to:

$$E = 1 - (1-E_S)(1-E_D), \quad (10)$$

where E_D and E_S are, respectively, the deposition efficiencies due to the individual mechanisms of diffusion and sedimentation over the pause period. The expressions for E_D and E_S are given by (Yu, 1978): (36)

$$E_D = 1 - \sum_{i=1}^{3} \frac{4}{\alpha_i} \exp(-\alpha_i^2 \tau_D)\left(1 - \sum_{i=1}^{3} \frac{4}{\alpha_i^2}\right) \exp\left[-\frac{4\tau_D^{1/2}}{\pi^{1/2}\left(1 - \sum_{i=1}^{3} \frac{4}{\alpha_i^2}\right)}\right],$$

where $\tau_D = D\tau/R^2$ in which τ is the pause time, and α_1, α_2, and α_3 are the first three roots of the equation:

$$J_0(\alpha) = 0, \quad (37)$$

in which J_0 is the Bessel function of the zeroth order, and:

$$E_S = 1.1094\tau_S - 0.1604\tau_S^2, \text{ for } 0 < \tau_S \leq 1, \quad (38)$$

and:

$$E_S = 1 - 0.0069\tau_S^{-1} - 0.0859\tau_S^{-2} - 0.0582\tau_S^{-3}, \text{ for } \tau_S > 1, \quad (39)$$

where

$$\tau_S = u_S\tau / 2R.$$

RESULTS

DEPOSITION IN HUMAN ADULTS (AGE 25 OR OLDER)

Extensive calculations were performed to predict the deposition pattern of diesel particles in the lungs of human adults under various exposure conditions. The respiratory cycle was assumed to consist of a sequence of inhalation, pause and exhalation, each with a respective duration fraction of 0.435, 0.05, and 0.515 of a breathing period. This is the breathing pattern suggested by the Task Group on Lung Dynamics (1966) for adults breathing naturally. The influence of various controlling factors on deposition was examined individually. The results are summarized below:

The Effect of Particle Characteristics

The characteristics that had the most effect on deposition were the mean particle size and the geometric standard deviation of the particle size distribution. Because of the size of the particles, most diesel particle deposition in the lung was through diffusion. Varying the particle density p from 0.8 to 2 g/cm^3 and the packing density ϕ from 0.2 to 0.5 resulted in only a minor effect on deposition.

Figure 1 shows total and regional deposition fractions calculated for mouth breathing in human adults using Weibel's lung model for particles with a MMAD between 0.1 and 0.3 μm, $\phi = 0.3$, $p = 1.5$ g/cm^3, and $\sigma_g = 4.5$, the latter representing the upper bound of measured values. In this figure, the deposition fraction for a specific region of the respiratory system is defined as the ratio of the mass of particles deposited in that region to the total mass of particles inhaled during a respiratory cycle. Total deposition (T) is the sum of regional deposition. It can be seen that increasing the MMAD increases deposition in the head region (H), but decreases deposition in both the tracheobronchial (TB) and alveolar regions (A). The increase or decrease in regional deposition, however, was small. As MMAD increased from 0.1 to 0.3 μm, alveolar deposition decreased from 13 percent to 10 percent. Increasing σ_g led to increases in both total and regional deposition (Figure 2). As σ_g increased from 1.5 to 4.5, alveolar deposition increased from 6 percent to 11 percent.

The Effect of Breathing Mode

Air passages in the head can filter inhaled particles and prevent them from entering the lung. Since the structure of air passages within the nose and mouth is different, particle deposition depends on the route of entry. Figure 3 shows the deposition of highly dispersed diesel particles ($\sigma_g = 4.5$) inhaled exclusively through the nose or mouth, or through a combination of both (half nose and half mouth). Although total deposition was markedly higher for pure nose breathing, the breathing mode had only a minor effect on tracheobronchial and alveolar deposition. If particles with a smaller σ_g (1.9) are considered, the depositional changes are even smaller.

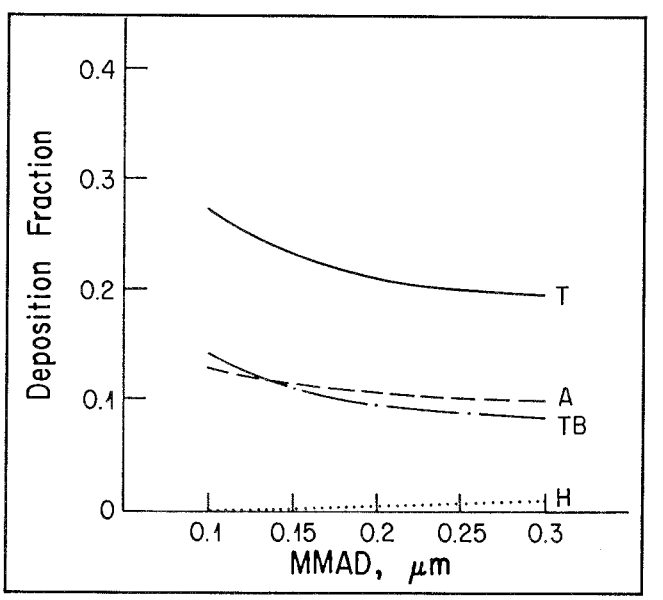

Figure 1. Total (T) and regional (head H, tracheobronchial TB, alveolar A) deposition of DEPs in human adults (age 25 or older) at mouth breathing. Conditions for calculation: (a) $\sigma_g = 4.5$, $\phi = 0.3$, and $p = 1.5$ g/cm^3, (b) lung volume (LV) = 3200 cm^3, (c) tidal volume (TV) = 500 cm^3 and respiratory frequency (RF) = 14 min^{-1}.

The Effect of Minute Ventilation

The dependence of deposition fraction on minute ventilation is shown in Figure 4. At a given respiratory frequency, deposition in the head and alveolar regions increased with

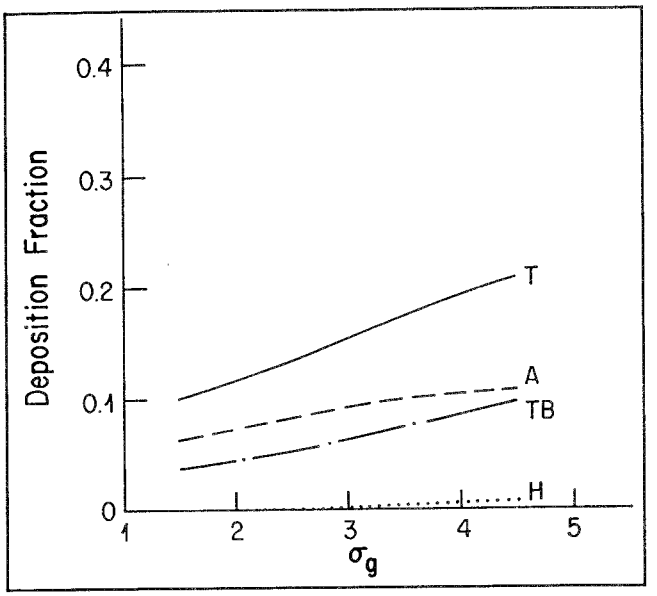

Figure 2. Total and regional deposition of DEPs in human adults at mouth breathing. Conditions for calculation: (a) MMAD = 0.2 μm, ϕ = 0.3, and p = 1.5 g/cm^3, (b) LV = 3200 cm^3, and (c) TV = 500 cm^3 and RF = 14 min^{-1}.

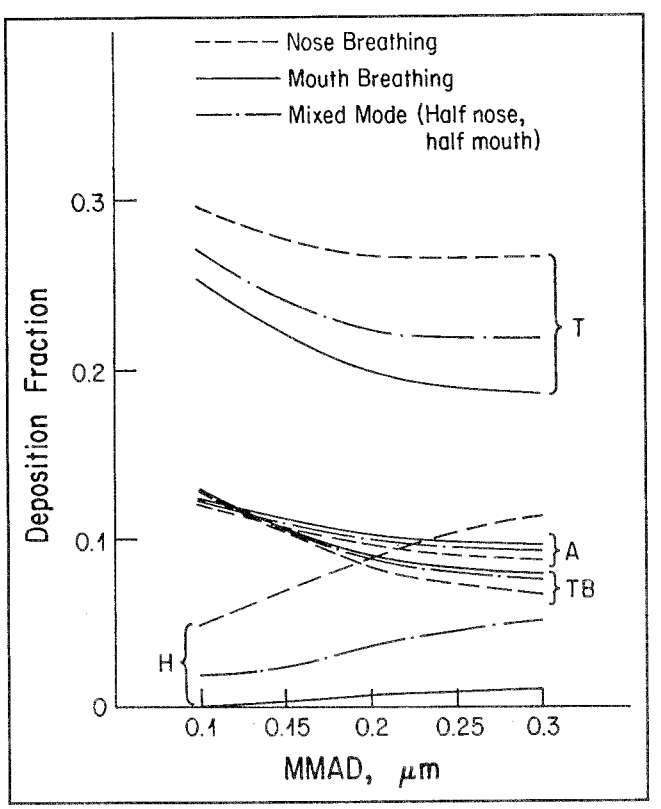

Figure 3. Total and regional deposition of DEPs in human adults at different breathing modes. Conditions for calculation: (a) σ_g = 4.5, ϕ = 0.3, and p = 1.5 g/cm^3, (b) LV = 3200 cm^3, and (c) TV = 500 cm^3 and RF = 14 min^{-1}.

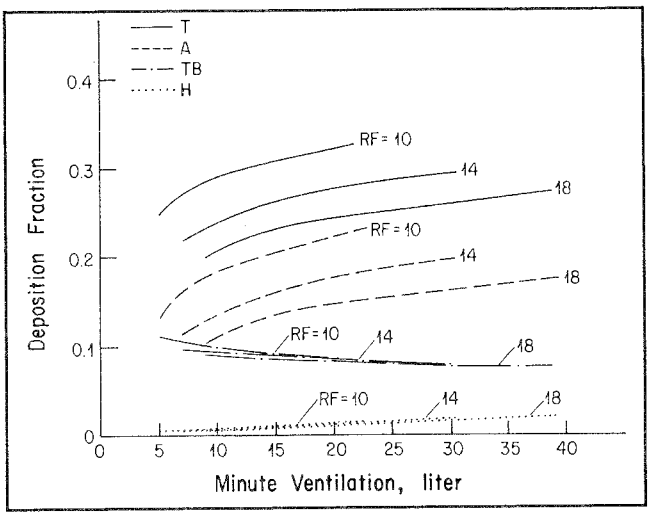

Figure 4. Total and regional deposition of DEPs in human adults at different ventilation conditions. Conditions for calculation: (a) MMAD = 0.2 μm, σ_g = 4.5, ϕ = 0.3, and p = 1.5 g/cm^3, (b) LV = 3200 cm^3, and (c) mouth breathing.

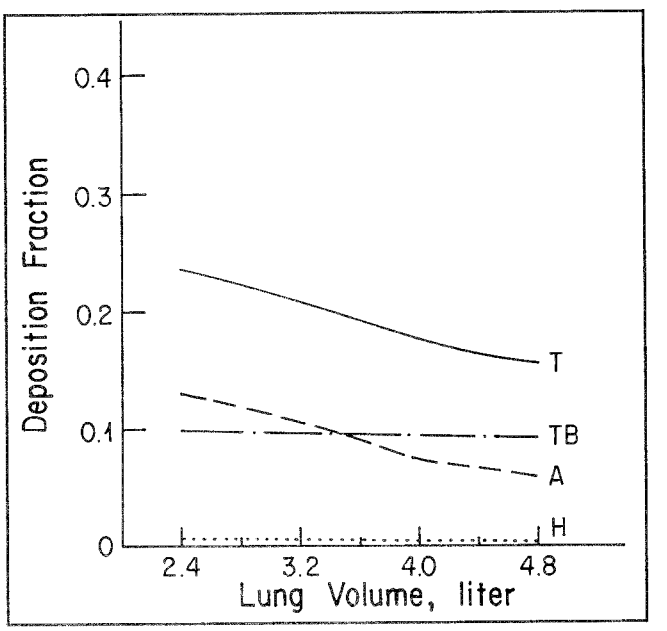

Figure 5. Total and regional deposition of DEPs in human adults with different lung volumes. Conditions for calculation: (a) MMAD = 0.2 μm, σ_g = 4.5, ϕ = 0.3, and p = 1.5 g/cm^3, (b) TV = 500 cm^3 and RF = 14 min^{-1}, and (c) mouth breathing.

minute ventilation while tracheobronchial deposition decreased. We also found that head and tracheobronchial deposition were nearly independent of respiratory frequency at a given minute ventilation. However, alveolar deposition was strongly dependent on respiratory frequency. The latter result is the fact that minute ventilation is the product of respiratory frequency and tidal volume. Decreasing the respiratory frequency at a given minute ventilation corresponds to an increase in tidal volume, which causes tidal air to penetrate more deeply into the lung and more particles to deposit in the alveoli.

Lung Models and Intersubject Variability

Deposition of diesel particles in the lungs depends upon the lung model chosen as well as the lung volume of a given lung model. Since lung volume and airway structure are distinct for every individual, the study of these factors may lead to useful insights into intersubject variabilities.

The variation of deposition fraction with respect to lung volume in Weibel's lung model is shown in Figure 5. We found that deposition decreased as lung volume increased, primarily in the alveolar region because of the decreasing amount of the tidal air that entered this region.

The depositions in different lung models are given in Table 3. Both regional and total deposition were found unaffected by the lung model chosen although alveolar deposition was significantly lower in Olson's model than the other models because of its larger tracheobronchial airway volume and fewer alveoli. The average total deposition for the four models was found to be 10.3 percent with a standard deviation of 1.79 percent.

Another factor which accounts for intersubject variability in lung deposition is the variability of deposition in the head region. Yu et al. (1981) have calculated the standard deviation of the head deposition efficiency from the deposition data in human adults (Equations (6)-(12)). Using these data, we calculated the deposition fractions of DEPs at nose breathing in the tracheobronchial and alveolar regions when the head deposition efficiency was varied by one standard deviation during both inspiratory and expiratory flows. The results are shown in Table 4. Although there was a significant difference in the head deposition when the nose deposition efficiency was increased or decreased, the deposition in the tracheobronchial and alveolar regions was changed only slightly.

Table 3. Effect of Lung Model on Deposition of Diesel Exhaust Particles[a]

Lung Model	Deposition Fraction (percent)			
	Head	Tracheobronchial	Alveolar	Total
Weibel	0	4.28	7.00	11.3
Olson et al.	0	3.74	3.44	7.28
Hansen and Ampaya	0	3.83	7.74	11.6
Yeh and Schum	0	3.54	7.55	11.1
Mean	0	3.85	6.43	10.3
Standard Deviation	0	0.23	1.76	1.79

(a) On the basis of the following conditions:
mass median aerodynamic diameter = 0.2 μm, σ_g = 1.9, ϕ = 0.3, and p = 1.5 g/cm^3;
lung volume = 3200 cm^3, tidal volume = 500 cm^3, respiratory frequency = 14 min^{-1};
mouth breathing.

Table 4. Effect of Nose Deposition Efficiency on Deposition of Diesel Exhaust Particles[a]

Nose Deposition Efficiency	Deposition Fraction (percent)			
	Head	Tracheobronchial	Alveolar	Total
Mean	4.37	4.25	6.94	15.6
Mean + One Standard Deviation	11.4	4.12	6.72	22.3
Mean − One Standard Deviation	3.12	4.28	7.00	11.6

(a) On the basis of the following conditions:
mass median aerodynamic diameter = 0.2 μm, σ_g = 1.9, ϕ = 0.3, and p = 1.5 g/cm^3;
lung volume = 3,200 cm^3, tidal volume = 500 cm^3, respiratory frequency = 14 min^{-1}.

DEPOSITION IN CHILDREN AND YOUNG ADULTS UNDER AGE 25

Lung deposition of diesel particles in young adults under age 25 was calculated for a typical particle condition of MMAD = 0.2 μm, σ_g = 1.9, ϕ = 0.3, and p = 1.5 g/cm^3. Since the breathing mode did not affect depositions in the tracheobronchial and alveolar regions in a significant way, we present only the results of nose breathing. For all ages, the respective duration fractions of inhalation, pause, and exhalation were assumed to be the same as for adults. The tidal volume and respiratory frequency used in the calculations were obtained from the empirical formulas of Hofmann (1982) for subjects at rest condition:

$$\text{Tidal Volume} = 21.7 + 35.15t - 0.64t^2, \ (\text{cm}^3) \quad (40)$$

and

$$\text{Respiratory Frequency} = 15.17/(0.25t + 0.5) + 11.75, \ (\text{min}^{-1}) \quad (41)$$

where t is age in years.

Figure 6 shows total and regional deposition as a function of age. With the exception of alveolar deposition at very early ages (less than two years old), both total and regional deposition of DEPs in children were higher than that of adults, particularly in the first eight years of life. Although head and tracheobronchial deposition decreased monotonically as age progressed, alveolar deposition peaked at about five years of age. This is a result of the combined scavenging effect of the head and tracheobronchial regions. Total deposition reached a maximum at the age of two years.

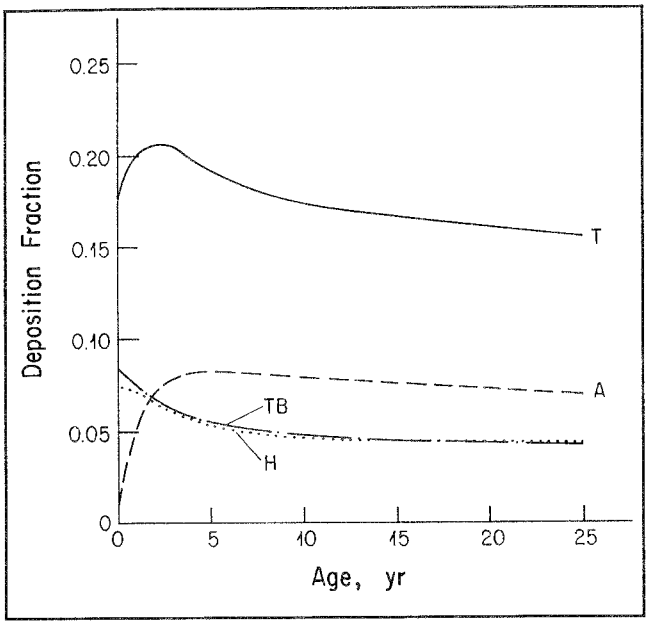

Figure 6. Total and regional deposition of DEPs in humans under age 25. Conditions for calculation: (a) MMAD = 0.2 μm, σ_g = 1.9, ϕ = 0.3, and p = 1.5 g/cm^3, and (b) nose breathing.

Figure 7 shows deposition fractions at the airway generation level for different age groups. The general deposition pattern was similar for all ages, with the maximum deposition per generation occurring in the alveolar region. This result is typical for diffusion-dominated particles. However, the deposition fraction per generation in the tracheobronchial region decreased with age.

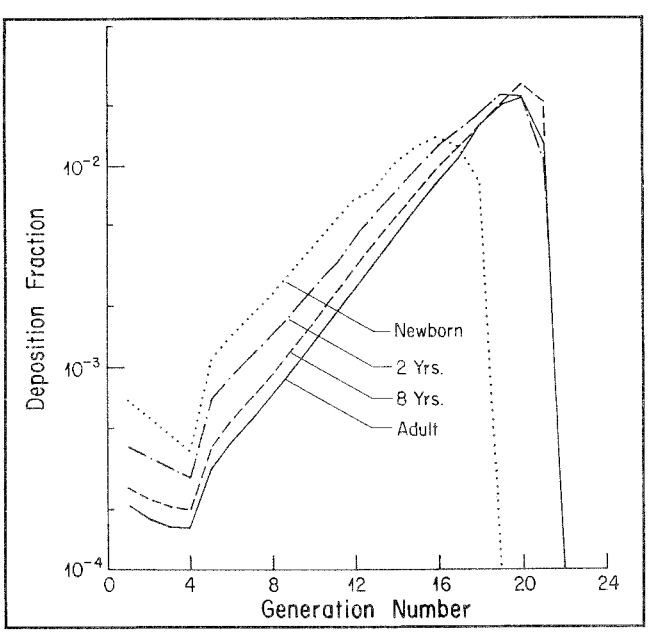

Figure 7. Deposition distribution patterns of DEPs in humans under age 25. Conditions for calculation: (a) MMAD = 0.2 μm, σ_g = 1.9, ϕ = 0.3, and p = 1.5 g/cm^3, and (b) nose breathing.

For a general comparison of lung exposure to diesel particles between different age groups exposed to the same concentration of particles, we calculated volumetric and surface minute doses defined below:

$$M = \frac{\text{mass of DEPs deposited in the lung per minute}}{\text{total lung volume}}, \quad (42)$$

$$M_1 = \frac{\text{mass of DEPs deposited in the lung per minute}}{\text{total airway surface area}}, \quad (43)$$

$$M_2 = \frac{\text{mass of DEPs deposited on the unciliated airways per minute}}{\text{surface area of the unciliated airways}}. \quad (44)$$

Table 5 shows the results of M, M_1, and M_2 at an exposure concentration of 1 mg/m^3. As can be seen, that M_2 increased up to the age of two years and then decreased, whereas M and M_1 appeared to decrease monotonically. The values of M and M_1 in newborns were three to four times higher than in adults and M_2 at two years of age was almost twice the adult's dose.

DEPOSITION IN LABORATORY ANIMALS

Until recently, no deposition data have been available for DEPs in humans. Limited measurements of the deposition of DEPs or similar aggregated particles have been made on rats and other laboratory species. Raabe et al. (1977) studied deposition in Long Evans rats and Chan et al. (1981) measured deposition in male Fischer 344 rats using DEPs tagged with radioactive tracers of ^{131}Ba and ^{14}C. More recently, Wolff et al. (1984) reported on the deposition of inhaled $^{67}Ga_2O_3$ particles in Fischer rats, beagle dogs, and mice.

To verify our deposition model for DEPs, we calculated deposition in rats under the experimental conditions stated. The respiratory cycle consisted of equal periods of inhalation and exhalation through the nose without pause. Table 6 compares our predictions with the experimental data. Predicted and experimental results agreed well in all cases.

COMPARISON OF DEPOSITION BETWEEN LABORATORY SPECIES AND HUMANS

To facilitate the extrapolation from one species to another, Figure 8 presents total and alveolar deposition of diesel particles calculated as a function of body weight. Despite the fact that the body weights of humans and laboratory species differ by several orders of magnitude, variations in deposition between humans and laboratory animals over a respiratory cycle were found to be within 30 percent. An increase in body weight was associated with a slight decrease in deposition. Figure 9 compares deposition fractions at airway generation level for Fischer rats and human adults. Again, deposition patterns were similar.

Table 5. Volumetric and Surface Minute Doses in Humans Under Age 25[a]

Age (year)	Lung Volume (cm^3)	Airway Surface Area ($10^3 cm^2$) total	Airway Surface Area ($10^3 cm^2$) unciliated	Minute Ventilation (cm^3/min)	M ($10^{-3}\mu g/min.cm^3$)	M_1 ($10^{-6}\mu g/min.cm^2$)	M_2 ($10^{-6}\mu g/min.cm^2$)
Newborn	83	0.0215	0.0202	914	1.025	3.958	0.369
1	211	0.0740	0.0724	1,798	1.087	3.098	1.286
2	338	0.118	0.116	2,405	0.998	2.913	1.505
4	592	0.192	0.189	3,331	0.795	2.450	1.454
8	1098	0.302	0.298	4,664	0.557	2.023	1.258
15	1972	0.454	0.450	6,197	0.383	1.665	1.059
25	3200	0.633	0.627	7,000	0.245	1.237	0.775

(a) On the basis of the following conditions:
mass median aerodynamic diameter = 0.2 μm, σ_g = 1.9, ϕ = 0.3, and ρ = 1.5 g/m^3;
particle concentration = 1 mg/m^3;
nose breathing.

Table 6. Deposition Predictions Compared to Experimental Data on Rats

Species	Particle Characteristics	Head (percent) Data	Head (percent) Prediction	Tracheobronchial (percent) Data	Tracheobronchial (percent) Prediction	Alveolar (percent) Data	Alveolar (percent) Prediction	Total (percent) Data	Total (percent) Prediction
Long Evans Rats	Aluminosilicate MMAD = 0.08-0.1μm σ_g = 1.5	4.7 ± 0.7[a]	5.4-5.6	6.9 ± 0.6[a]	4.7-5.5	20.7 ± 1.7[a]	19.5-22.0	31.8 ± 2.6[a]	30.1-33.5
Fischer 344 Rats	DEPs MMAD = 0.01-0.15μm σ_g = 1.8-1.9	N.A.	6.0-6.8	4[b]	3.1-4.6	11[b]	10.3-13.4	15-17[b]	13.5-17.9
Fischer 344 Rats	$^{67}Ga_2O_3$ MMAD = 0.10 ± 0.02μm σ_g = 1.6	9[c]	6.8-7.5	5[c]	2.2-3.1	10-11[c]	6.7-9.3	25[c]	16.5-19.2

(a) Raabe et al. (1977).
(b) Cban et al. (1981).
(c) Wolff et al. (1984).

Table 7. Volumetric and Surface Minute Doses for Various Species[a]

Species	Body Weight (g)	Lung Volume (cm^3)	Airway Surface Area ($10^3 cm^2$) Total	Airway Surface Area ($10^3 cm^2$) Unciliated	Minute Ventilation (cm^3/min)	M ($10^{-3}\mu g/min.cm^3$)	M_1 ($10^{-6}\mu g/min.cm^2$)	M_2 ($10^{-6}\mu g/min.cm^2$)
Hamster	130	2.28	2.619	2.605	67	3.548	3.088	2.382
Fischer Rat	250	4.16	4.124	4.095	156.8	3.434	3.463	2.608
Guinea Pig	600	8.39	9.591	9.472	242.5	4.056	3.548	1.994
Human	70,000	3,200	633	627	7,000	0.249	1.237	0.775

(a) On the basis of the following conditions:
mass median aerodynamic diameter = 0.2μm, σ_g = 1.9, ϕ = 0.3, and ρ = 1.5 g/cm^3;
particle concentration = 1 mg/m^3;
nose breathing.

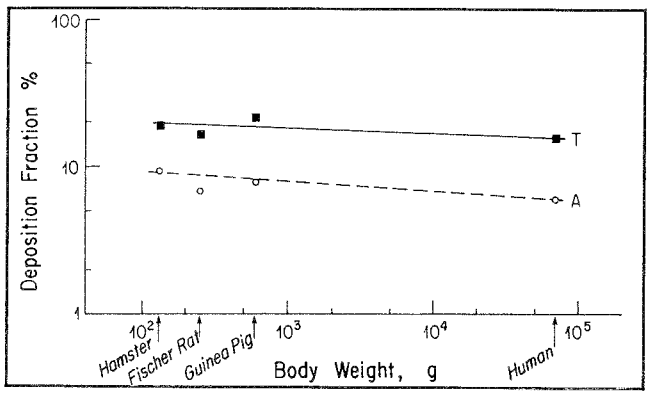

Figure 8. Total and alveolar deposition of DEPs in human adults and laboratory species. Conditions for calculation: (a) MMAD = 0.2 μm, σ_g = 1.9, ϕ = 0.3, and p = 1.5 g/cm^3, and (b) nose breathing.

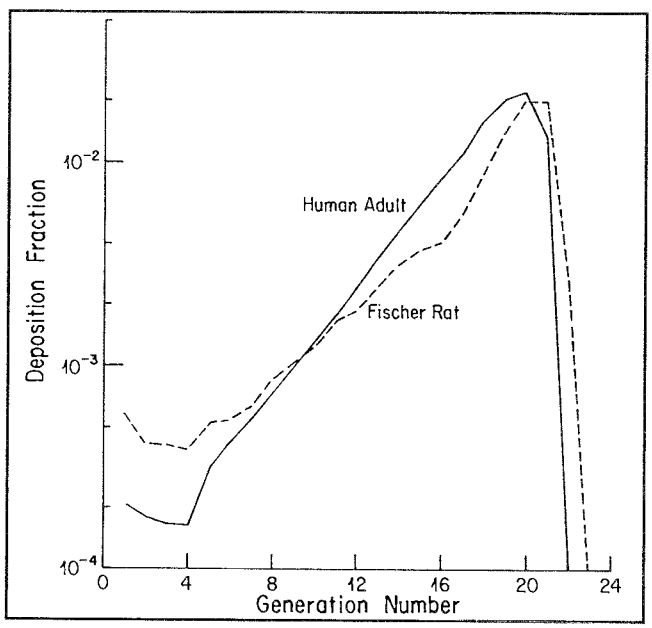

Figure 9. Comparison of deposition distribution patterns of DEPs between human adults and Fischer rats. Conditions for calculation: (a) MMAD = 0.2 μm, σ_g = 1.9, ϕ = 0.3, and p = 1.5 g/cm^3, and (b) nose breathing.

The results of M, M_1, and M_2 for different species exposed to 1 mg/m^3 of DEPs are shown in Table 7. Typically, the minute dose of laboratory species was found to be higher than that of humans because of the higher respiratory frequency and smaller lungs of laboratory animals. For Fischer rats, the surface minute dose of unciliated airways was three to four times greater than that of a human adult.

SUMMARY AND CONCLUSIONS

Our principal objective was to determine the deposition pattern of inhaled DEPs in the lungs of humans and laboratory species. The potentially hazardous effects of these particles are closely associated with the dose of particles deposited in the lung. We hope that the information obtained from this study will enhance understanding of the dose-response relationship and establish a quantitative basis for interspecies extrapolation.

For obvious reasons, experimental deposition studies of DEPs in the lungs have been limited to laboratory species. The theoretical studies undertaken in this project were designed to verify previous experimental data and to provide information about deposition in human lungs, including those of children and young adults. The manner in which deposition was affected by various factors such as particle characteristics, lung geometry, and ventilation conditions, were examined in great detail.

For the size range of DEPs, we found that the fraction of particles that deposits in various regions of the respiratory tract did not strongly depend on particle characteristics. For human adults breathing through the nose, we estimated that about ten percent of inhaled DEPs deposit in the head, tracheobronchial region, and in the alveoli.

Our calculation of deposition in human adults also indicated that switching from nose to mouth breathing decreased deposition levels in the head, but did not markedly affect tracheobronchial and alveolar deposition. However, increasing the tidal volume or minute ventilation at a fixed breathing rate significantly increased alveolar deposition, although increases in head and tracheobronchial deposition were only minor.

Calculated deposition was relatively insensitive to the lung models used, indicating that intersubject variability may be minimal with regard to deposition of DEPs. The coefficient of variation (standard deviation/mean) for total deposition was approximately 0.17.

Both lung morphometry and ventilation conditions vary during postnatal growth. Deposition of DEPs was greater in children than in adults. The surface minute dose in the unciliated airways reached a maximum in the two-year-old children where the dose was approximately twice that of an adult. Thus, it may be inferred that children are more susceptible to DEPs than adults.

Deposition studies in animals showed that lung deposition efficiency was slightly higher in small animals than in humans. Volumetric and surface minute doses were also higher for small animals. In unciliated airways, the surface minute dose for Fischer rats was three to four times greater than that of humans.

ACKNOWLEDGMENTS

We are grateful to Dr. L. Gradon for discussions about the chemical composition of DEPs, to B. Asgharian for his technical assistance, and to J. Helfer for his assistance in preparing this report.

REFERENCES

Angus GE, Thurlbeck WM, 1972. Number of alveoli in the human lung. J Appl Physiol; 32:483-485.

Barth DS, Blacker SM, 1978. The EPA program to assess the public health significance of diesel emissions. J Air Pollut Control Assoc; 28:768-771.

Boersma H, Frans PGM, Linden VD, Prahl-Andersen B, 1979. Physical growth and dental development. In: Prahl-Andersen B, Kowalski CJ, Heydendael PHJM, eds. A mixed-longitudinal interdisciplinary study of growth and development. New York: Academic Press, pp. 541-543.

Boyden EA, Tompsett DH, 1965. The changing patterns in the developing lungs of infants. Acta Anat; 61:164-192.

Chan TL, Lee PS, Hering WE, 1981. Deposition and clearance of inhaled diesel exhaust particles in the respiratory tract of Fisher rats. J Appl Toxicol; 1:77-82.

Chan TL, Lee PS, Hering WE, 1984. Pulmonary retention of inhaled diesel particles after prolonged exposure to diesel exhaust. Fundam Appl Toxicol; 4:624-631.

Chan TL, Yu CP, 1982. Charge effects on particle deposition in the human tracheobronchial tree. Ann Occup Hyg; 11:65-75.

Cheng YS, Yeh HC, Mauderly JL, Mokler BV, 1984. Characterization of diesel exhaust in a chronic inhalation study. Am Ind Hyg Assoc J; 45:547-555.

Davies CN, 1945. Definite equations for the fluid resistance of spheres. Proc Phys Soc; 57:259-270.

Davies G, Reid L, 1970. Growth of the alveoli and pulmonary arteries in children. Thorax; 25:669-681.

Diu CK, Yu CP, 1983. Respiratory tract deposition of polydisperse aerosols in humans. Am Ind Hyg Assoc J; 44:62-65.

Dolan DF, Kittelson DB, 1979. Roadway measurements of diesel exhaust aerosols. SAE Technical paper 790492.

Dunnill MS, 1962. Postnatal growth of the lung. Thorax; 17:329-333.

Engel S, 1950. Die lunge des kindes. Stuttgart, Georg Thieme Verlag.

Engel S, 1962. Lung Structure. Springfield, Illinois: Thomas, pp. 145-154.

Godfrey S, 1974. Growth and development of the respiratory system. In: Davis JA, Dobbing J, eds. Scientific Foundations of Paediatrics. London: Heinemann, pp. 254-271.

Gross KB, 1981. Pulmonary function testing of animals chronically exposed to diluted diesel exhaust. J Appl Toxicol; 1:116-123.

Hansen JE, Ampaya EP, 1975. Human air space, shapes, sizes, areas and volumes. J Appl Physiol; 38:990-995.

Harris RJ, Jr Fraser DA, 1976. A model for deposition of fibers in the human respiratory system. Am Ind Hyg Assoc J; 37:73-89.

Heinrich U, Mohr U, Pott F, Stober W, 1985. Carcinogenesis in rodents after long-term high dose inhalation studies with diesel exhaust emissions. Paper 8E1, presented at AAAR Meeting, Nov. 18-22, Albuquerque, NM.

Hofmann W, 1982. Mathematical model for the postnatal growth of the human lung. Respir Physiol; 49:115-129.

Ingham DB, 1975. Diffusion of aerosols from a stream flowing through a cylindrical tube. J Aerosol Sci; 6:125-132.

Kasper G, 1982. Dynamics and measurement of smokes I. Aerosol Sci Tech; 1:187-199.

Kittelson DB, Dolan DF, 1980. Diesel exhaust aerosols. In: Willeke K, ed. Generation of aerosols and facilities for exposure experiments. Ann Arbor, Michigan: Ann Arbor Science, pp. 337-359.

Landahl HD, 1963. Particle removal by the respiratory system—note on the removal of airborne particulates by the human respiratory tract with particular reference to the role of diffusion. Bull Math Biophys; 25:29-39.

Lee PS, Chan TL, Hering EW, 1983. Long-term clearance of inhaled diesel exhaust particles in rodents. J Toxicol Environ Health; 12:801-813.

Mauderly JL, Jones RD, McClellan RO, Henderson RF, 1985. Late-occurring effects in rats chronically exposed to diesel exhaust. Paper 8E3, presented at AAAR Meeting, Nov. 18-22, Albuquerque, NM.

McCain JD, Drehmel DC, 1981. Particle size measurements of automotive diesel emissions. Environ Int; 6:423-426.

Morrow PE, Yu CP, 1985. Models of aerosol behavior in airways. In: Moren F, Newhouse MT, Dolovich MB, eds. Aerosols in Medicine. Principles, Diagnosis and Therapy. New York: Elsevier, pp. 149-191.

Olson DE, Dart GA, Filley GF, 1970. Pressure drop and fluid flow regime of air inspired into the human lung. J Appl Physiol; 28:482-494.

Phalen RF, Oldham MJ, Beaucage CB, Crocker TT, Mortensen JD, 1985. Postnatal enlargement of human tracheobronchial airways and implications for particle deposition. Anat Rec; 212:368-380.

Pich J, 1972. Theory of gravitational deposition of particles from laminar flows in channel. J Aerosol Sci; 3:351-361.

Raabe OG, Yeh HC, Newton GJ, Phalen RF, Velasquez DJ, 1977. Deposition of inhaled monodisperse aerosols in small rodents. In: Walton WH, ed. Inhaled Particles IV. Oxford, England: Pergamon Press, pp. 3-21.

Reid L, 1977. The lung: Its growth and remodeling in health and disease. Am J Roentg; 129:777-788.

Schreider JP, Hutchens JO, 1979. Particle deposition in the guinea pig respiratory tract. J Aerosol Sci; 10:599-607.

Schum GM, Yeh HC, 1980. Theoretical evaluation of aerosol deposition in anatomical models of mammalian lung airways. Bull Math Biol; 42:1-15.

Soderholm SC, 1981. Physical characterization of diesel exhaust particles in exposure chambers. Environ Int; 5:325-330.

Stahl WR, 1967. Scaling of respiratory variables in mammals. J Appl Physiol; 22:453-459.

Synder WS, 1975. Report of Task Group on Reference Man. Oxford, England: Pergamon Press, pp. 151-173.

Task Group on Lung Dynamics, 1966. Deposition and retention models for internal dosimetry of the human respiratory tract. Health Phys; 12:173-207.

Testut JL, 1922. Traite de l'anatomie humaine; Vol. 3.

Thurlbeck WM, Angus GE, 1975. Growth and aging of the normal human lung. 17th Aspen Lung Conference, Chest 67 (Supplement); 3-7.

Waller RE, 1980. Trends in lung cancer in London in relation to exposure to diesel fumes. In: Pepelko WE, Danner RM, Clarke NA, eds. Health Effects of Diesel Engine Emissions. US EPA-600/9-80-0576, pp. 1085-1099.

Weibel ER, 1963. Morphometry of the human lung. Berlin, Germany: Springer-Verlag.

Wolff RK, Kanapilly GM, Gray RH, McClellan RO, 1984. Deposition and retention of inhaled aggregates $^{67}Ga_2O_3$ particles in Beagle dogs, Fischer 344 rats, and CD-1 mice. Am Ind Hyg Assoc J; 45:377-381.

Yeh HC, Schum GM, 1980. Models of human lung airways and their application to inhaled particle deposition. Bull Math Biol; 42:461-480.

Yu CP, 1978. Exact analysis of aerosol deposition during steady breathing. Powder Tech; 21:55-62.

Yu CP, Diu CK, 1982. A comparative study of aerosol deposition in different lung models. Am Ind Hyg Assoc J; 43:54-65.

Yu CP, Diu CK, 1983. Total and regional deposition of inhaled aerosols in humans. J Aerosol Sci; 5:599-609.

Yu CP, Diu CK, Soong TT, 1981. Statistical analysis of aerosol deposition in nose and mouth. Am Ind Hyg Assoc J; 42:726-733.

APPENDIX A — MATHEMATICAL MODEL OF THE HUMAN LUNG POSTNATAL DEVELOPMENT

INTRODUCTION

Morphometric data for children's lungs has been reported in the literature by many investigators. There appears to be general agreement that the full number of bronchial airways are present at birth and that alveolization of bronchioles continues postnatally in a proximal direction. However, there is considerable controversy regarding the details of lung growth. The mathematical model developed in this study was based upon the morphometric data available. A special effort was made to ensure that the model was consistent with all major measurements.

NUMBER OF AIRWAYS AND ALVEOLI

The model assumed that an adult's lung is patterned after Weibel's model and that full growth is achieved at age of 25 years. By the dichotomous branching airway structure of Weibel's model, the number of airways $N_i(t)$ at generation i for age t was required to assume the following form:

$$N_i(t) = 2^i, \qquad \text{for } 0 \le i \le 20 \qquad \text{(A-1)}$$

$$\begin{cases} N_{21}(t) = N_r(t), \\ N_{22}(t) = N_{23}(t) = 0, \end{cases} \qquad \text{for } N_r(t) \le 2^{21} \qquad \text{(A-2)}$$

$$\begin{cases} N_{21}(t) = 2^{21}, \\ N_{22}(t) = N_r(t) - 2^{21}, \\ N_{23}(t) = 0, \end{cases} \qquad \text{for } 2^{21} < N_r(t) \le 2^{22} \qquad \text{(A-3)}$$

$$\begin{cases} N_{21}(t) = 2^{21}, \\ N_{22}(t) = 2^{22}, \\ N_{23}(t) = N_r(t) - 2^{22} - 2^{21}, \end{cases} \qquad \text{for } N_r(t) > (2^{21} + 2^{22}) \qquad \text{(A-4)}$$

where $N_r(t)$ is the total number of airways in the last three airway generations. The data for $N_r(t)$ was reported by Weibel (1963) and Dunnill (1962) and is shown in Figure A-1. It can be seen that $N_r(t)$ increases from approximately 1.5 million at birth to about 15 million at 8 years of age and remains nearly constant thereafter. The empirical equation which best fits the available data is shown below:

$$N_r(t) = \begin{cases} 2.036\text{x}10^7(1 - 0.926e^{-0.15t}), & t \le 8 \\ 1.468\text{x}10^7, & t > 8 \end{cases} \qquad \text{(A-5)}$$

Equations (A-2) to (A-4) imply that in the last 3 generations, the airways in the subsequent generation begin to appear only when those in the preceding generation have completed development.

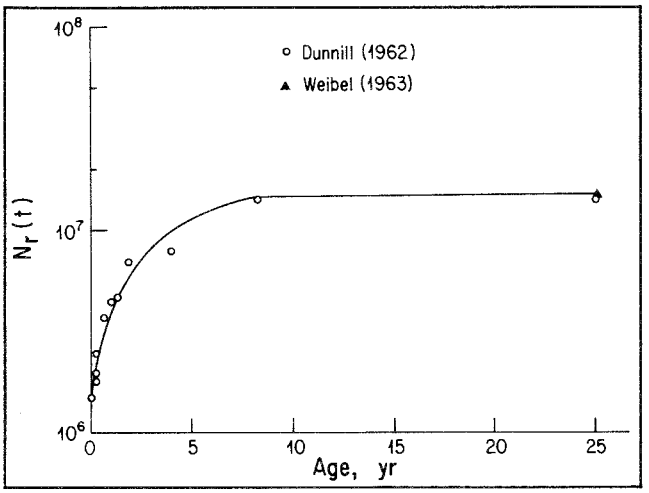

Figure A-1. Total number of airways in the last three generations as a function of age. The data points are from different authors and the solid line represents Equation (A-5).

The total number of alveoli during postnatal growth, $N_A(t)$, has also been measured by various investigators (Weibel, 1963; Dunnill, 1962; Angus and Thurlbeck, 1972). The results are shown in Figure A-2. The empirical equation which best fits the observed data is found in the following form:

$$N_A(t) = 2.985\text{x}10^8(1 - 0.919e^{-0.45t}). \qquad \text{(A-6)}$$

The number of alveoli distributed in the unciliated airways at the airway generation level was determined by assuming that alveolization of airways took place sequentially in a proximal direction. For each generation, alveolization was considered to be complete when the number of alveoli in that generation reached the number determined by Weibel's model.

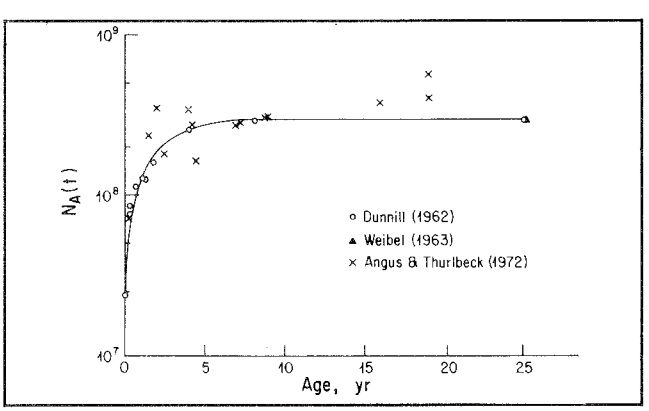

Figure A-2. Total number of alveoli as a function of age. The data points are from different authors and the solid line represents Equation (A-6).

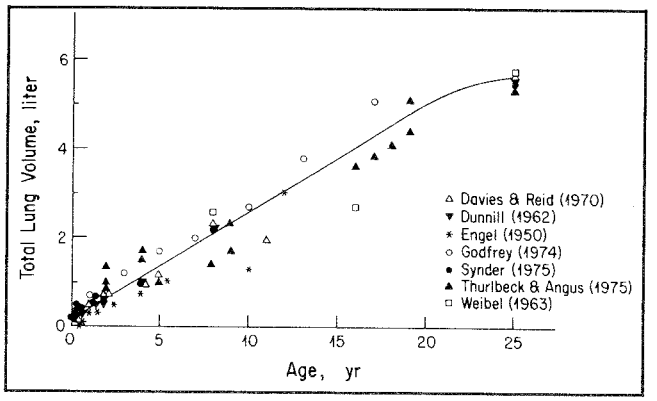

Figure A-3. Total lung volume as a function of age. The data points are from different authors and the solid line represents Equation (A-7).

AIRWAY SIZE

Four sets of data were used in the determination of airway size during postnatal growth: (1) total lung volume as a function of age, (2) airway size as given by Weibel's model, (3) the growth pattern of the bronchial airways, and (4) variation in alveolar size with age. The growth, with age, of total lung volume (TLV) including air, blood, and tissues, has been measured and recorded by many investigators (Weibel, 1963; Engel, 1950; Davies and Reid, 1970; Godfrey, 1974; Synder, 1975; Thurlbeck and Angus, 1975). Figure A-3 shows this data. The best fitting empirical equation was found to be:

$$TLV(t) = 1.15\text{x}10^5(1 - 0.998e^{-0.002}t). \quad (cm^3) \qquad (A\text{-}7)$$

Measurements have shown that the percentage of total lung volume occupied by tissue and blood remains nearly constant during postnatal life (Hofmann, 1982). It was therefore reasonable to derive the lung air volume from the data on total lung volume. Normalized to Weibel's model at a lung air volume of 4,800 cm^3 for an adult, the following equation was derived for the lung air volume, LV(t), for a child at age t:

$$LV(t) = 0.959\text{x}10^5(1 - 0.998e^{-0.002}t). \quad (cm^3) \qquad (A\text{-}8)$$

The growth pattern of the bronchial airways from the trachea to the 8th generation airways has been measured by Phalen et al. (1985) from 20 replica airway casts of the right upper lobe of the lung. The casts represented ages ranging from 11 days to 21 years old. The airway diameter D_i and length L_i at generation i were found to be linear functions of the body height, H(t). The equations for D_i and L_i, consistent with Weibel's model, can be expressed in the following form:

$$D_i(t) - D_{iw} = \alpha_i\,[H(t) - H(25)], \qquad (A\text{-}9)$$

$$L_i(t) - L_{iw} = \beta_i\,[H(t) - H(25)], \qquad (A\text{-}10)$$

where D_{iw} and L_{iw} are, respectively, the airway diameter and airway length corresponding to Weibel's model, α_i and β_i are the measured slopes, and H(t) is given by the equation:

$$H(t) = 1.82\text{x}10^2\,(1 - 0.725e^{-0.14}t), \ (cm) \qquad (A\text{-}11)$$

which was derived from the experimental data of Phalen et al. (1985) and Dunnill (1962) and shown in Figure A-4.

For estimating the growth pattern of the bronchial airways beyond the 8th generation, the values of α_i and β_i were extrapolated using the following equations:

$$\alpha_i = 3.26\text{x}10^{-2}\exp[-1.183\,(i+1)^{0.5}], \qquad (A\text{-}12)$$

$$\beta_i = 1.05\text{x}10^{-6}\exp[10.1\,(i+1)^{-0.2}]. \qquad (A\text{-}13)$$

Figure A-5 shows the results of α_i and β_i. It is clear from this figure that both α_i and β_i decrease as i increases and that β_i is always greater than α_i for any given airway generation. Thus, the growth of the bronchial airways is not uniform, which suggests that airway length grows at a faster rate than airway diameter and large airways grow faster than small airways.

There is no information available on the growth pattern of the airways in the alveolar region. We assumed that the size of airways including alveoli increase uniformly with age such that:

$$\frac{D_i}{D_{iw}} = \frac{L_i}{L_{iw}} = \frac{D_a}{D_{aw}} = f(t), \quad \text{for } 17 \le i \le 23 \qquad (A\text{-}14)$$

where D_a is the diameter of an alveolus at age t, $D_{aw} = 0.0288$ cm is the alveolar diameter for adults in accordance with Weibel's model, and f(t) is a function to be determined.

We assumed that all airways have cylindrical geometry and that the alveolar volume is 5/6 that of a sphere of diameter D_a. The lung air volume at any age t, LV(t), then takes the form:

$$LV(t) = \sum_{i=0}^{16} \frac{\pi}{4} D_i^2(t)L_i(t)N_i(t) + \sum_{i=17}^{23} \frac{\pi}{4} D_i^2(t)L_i(t)N_i(t) + \frac{5\pi}{36} D_a^3(t)N_A(t). \qquad (A\text{-}15)$$

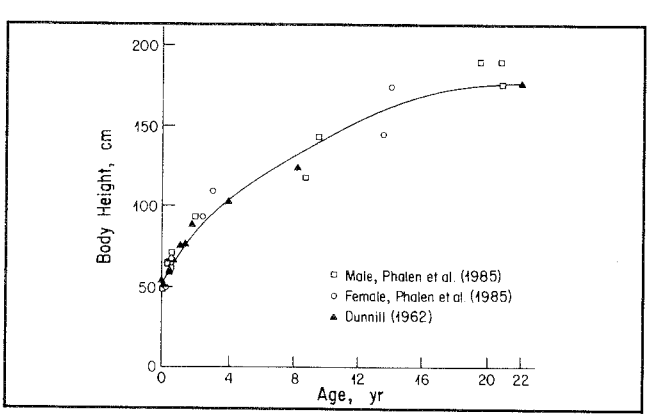

Figure A-4. Body height as a function of age. The data points are from different authors and the solid line represents Equation (A-11).

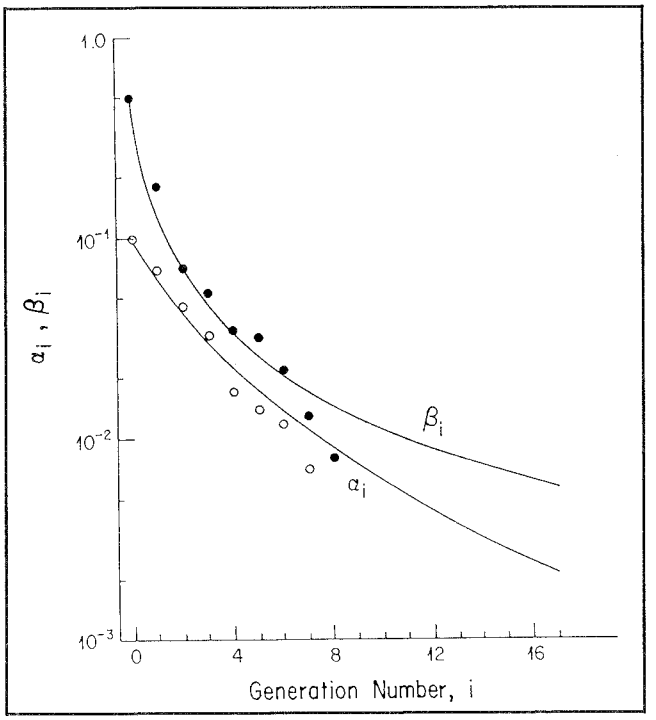

Figure A-5. Values of α_i and β_i for the ith airway generation. The data points are from Phalen et al. (1985) and the solid lines represent Equations (A-12) and (A-13).

Substituting Equations (A-1)-(A-4), (A-6), (A-8)-(A-10) and (A-14) into Equation (A-15) and making use of Equations (A-5) and (A-11), we obtained the following expression for f(t):

(A-16)

$$f(t) = \sqrt[3]{\frac{\left\{ LV(t) - \sum_{i=0}^{16} \frac{\pi}{4} D_i^2(t)\, L_i(t)\, N_i(t) \right\}}{\left\{ \sum_{i=17}^{23} \frac{\pi}{4} D_{iw}^2\, L_{iw} N_i(t) + \frac{5\pi}{36} D_{aw}^3\, N_A(t) \right\}}}\,.$$

Figure A-6 compares the calculated result of $D_a(t)$ using Equations (A-14) and (A-16) and the data of $D_a(t)$ reported by various investigators (Dunnill, 1962; Testut, 1922; Engel, 1962; Boyden and Tompsett, 1965). Despite the large scatter of data, there is a general agreement between the model prediction and the growth data over the entire range of postnatal enlargement.

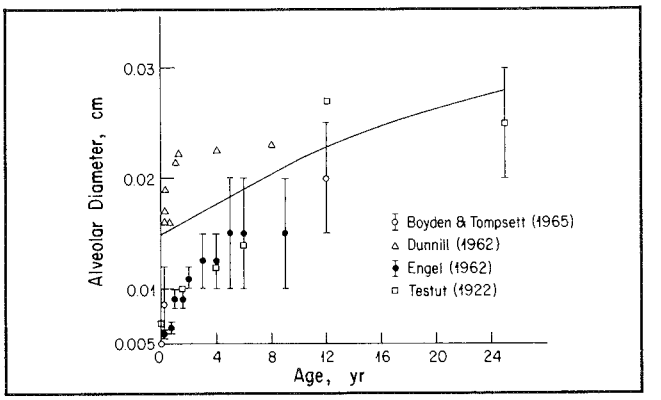

Figure A-6. Alveolar diameter as a function of age. The data points are from different authors and the solid line represents the calculated result.

APPENDIX B — LUNG MODELS FOR RATS, HAMSTERS, AND GUINEA PIGS

Morphometric data on the lung airways of rats, hamsters, and guinea pigs are listed in Tables B.1 through B.3 respectively. Data for rats were taken from the Whole Lung Anatomical Model reported by Schum and Yeh (1980). Since the airway dimensions of this rat lung model correspond to a total lung capacity of 13.73 cm^3, which is representative of Long Evans Rats, application of this model to Fischer rats required that the airway dimensions be scaled down by assuming the total lung capacity to be proportional to the body weight of the species. For hamsters and guinea pigs, data reported earlier by Schum and Yeh (1980) and Schreider and Hutchens (1979) were used. In order to compare the airway structure of these various laboratory species with humans, their morphometric data were plotted in Figures B-1 to B-4 by scaling the linear dimension of the lung with respect to body weight to the one-third power. Figure B-1 shows that rats and hamsters have fewer numbers of airways than humans at each airway generation, while the total number of airway generations are approximately the same. However, for guinea pigs there are more airways per generation, but the total number of generations is much less. Figures B-2 to B-4 show the relative size of airways when scaled according to body weight. It is seen that guinea pigs have smaller airway diameters at a given generation but longer airway paths than the other species; rat, hamster, and human airway sizes appear to be very similar in all respects.

Table B-1 Lung Model for Rats at Total Lung Capacity

Generation Number	Number of Airways	Length cm	Diameter cm	Accumulated Volume[b] cm^3
1	1	2.680	0.340	0.243
2	2	0.715	0.290	0.338
3	3	0.400	0.263	0.403
4	5	0.176	0.203	0.431
5	8	0.208	0.163	0.466
6	14	0.117	0.134	0.489
7	23	0.114	0.123	0.520
8	38	0.130	0.112	0.569
9	65	0.099	0.095	0.615
10	109	0.091	0.087	0.674
11	184	0.096	0.078	0.758
12	309	0.073	0.070	0.845
13	521	0.075	0.058	0.948
14	877	0.060	0.049	1.047
15	1477	0.055	0.036	1.141
16[a]	2487	0.035	0.020	1.185
17	4974	0.029	0.017	1.254
18	9948	0.025	0.016	1.375
19	19896	0.022	0.015	1.595
20	39792	0.020	0.014	2.003
21	79584	0.019	0.014	2.607
22	159168	0.018	0.014	4.389
23	318336	0.017	0.014	7.554
24	636672	0.017	0.014	13.784

(a) Terminal bronchioles.
(b) Including the attached alveolar volume (number of alveoli = 3×10^7, alveolar diameter = 0.0086 cm).

Table B-2 Lung Model for Hamsters at Total Lung Capacity

Generation Number	Number of Airways	Length cm	Diameter cm	Accumulated Volume[b] cm^3
1	1	1.6000	0.2600	0.085
2	2	0.6100	0.2400	0.140
3	3	0.3980	0.2200	0.186
4	4	0.1600	0.1960	0.205
5	7	0.2290	0.1570	0.236
6	12	0.1650	0.1250	0.260
7	21	0.1220	0.1000	0.280
8	34	0.1130	0.0780	0.299
9	56	0.0770	0.0730	0.317
10	93	0.0860	0.0716	0.348
11	154	0.0750	0.0620	0.382
12	254	0.0760	0.0490	0.419
13	420	0.0550	0.0410	0.469
14	695	0.0580	0.0320	0.482
15[a]	1150	0.0400	0.0270	0.513
16	2300	0.0320	0.0230	0.552
17	4600	0.0270	0.0200	0.610
18	9200	0.0230	0.0170	0.700
19	18400	0.0200	0.0150	0.848
20	36800	0.0180	0.0130	1.098
21	73600	0.0160	0.0120	1.558
22	147200	0.0140	0.0110	2.397
23	294400	0.0130	0.0100	3.986
24	588800	0.0120	0.0100	7.053

(a) Terminal bronchioles.
(b) Including the attached alveolar volume (number of alveoli = 3×10^7, alveolar diameter = 0.0069 cm).

Table B-3 Lung Model for Guinea Pigs at Total Lung Capacity

Generation Number	Number of Airways	Length cm	Diameter cm	Accumulated Volume[b] cm^3
1	1	4.5	0.30	0.32
2	2	1.2	0.22	0.404
3	5	1.9	0.16	0.594
4	17	0.85	0.10	0.704
5	86	0.53	0.065	0.884
6	312	0.26	0.050	1.014
7	1000	0.19	0.040	1.204
8	3000	0.10	0.030	1.414
9	9500	0.066	0.023	1.664
10[a]	42000	0.045	0.014	1.954
11	130000	0.024	0.009	2.714
12	250000	0.024	0.007	4.024
13	500000	0.024	0.006	6.244
14	1000000	0.024	0.006	10.684
15	2000000	0.032	0.005	20.975

(a) Terminal bronchioles.
(b) Including the attached alveolar volume (number of alveoli = 8.2×10^7, alveolar diameter = 0.008 cm).

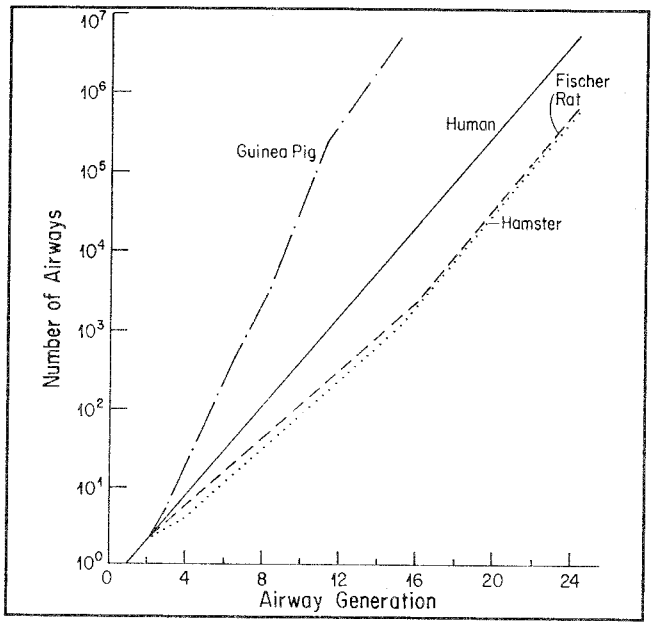

Figure B-1. Number of airways per generation for various species.

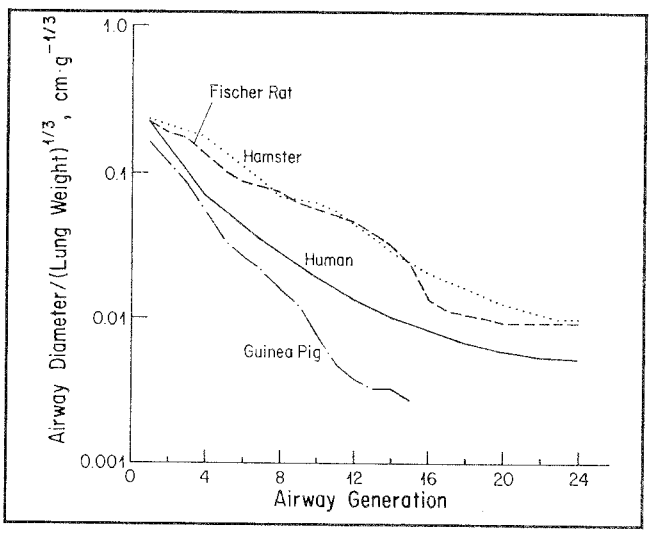

Figure B-2. Normalized airway diameter versus generation number for various species.

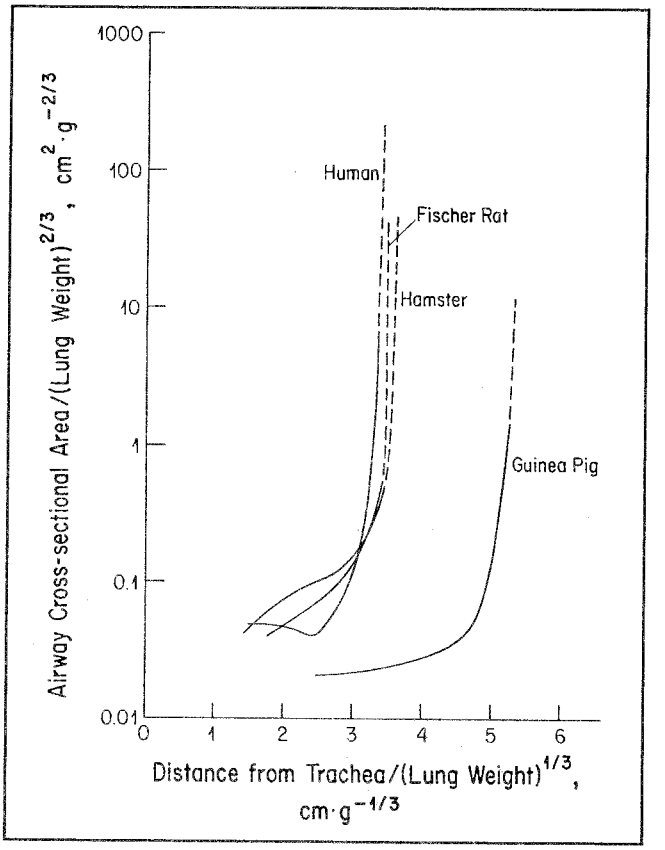

Figure B-3. Normalized airway cross-sectional area as a function of airway depth for various species. Dotted lines indicate the unciliated airways.

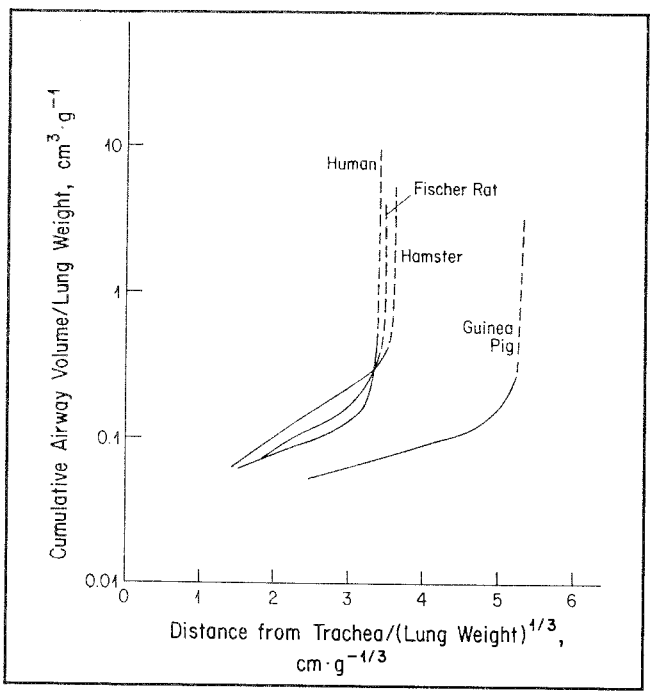

Figure B-4. Normalized cumulative airway volume as a function of airway depth for various species. Dotted line indicates the unciliated airways.

HEALTH REVIEW COMMITTEE'S REPORT

HEI OBJECTIVES

JUSTIFICATION FOR THE STUDY BY HEI

A central concern of the HEI relates to the health effects from inhaled particles and gases from mobile source emissions. Considerable attention has been given to the evaluation of biological responses caused by emission products, but less effort has been devoted to the quantification of dose. Without an accurate measurement of the dose, preferably at the site of action, descriptions of responses are of diminished value. Dr. Yu's project addresses several important issues regarding improved quantification of dose from known concentrations of atmospheric particulate matter. By focusing first on a specific category of automotive-derived particles, diesel exhaust particulate, Dr. Yu is able to characterize those aerosol properties (such as the mass median aerodynamic diameter* and size distribution) that influence regional deposition. After formulating a mathematical deposition model, Dr. Yu calculates and compares the deposition of inhaled diesel exhaust particulate in laboratory animals and in humans of different ages.

Once Dr. Yu's model has been fully developed and validated, it has several potential applications that are of interest to the HEI. Such applications include: Prediction of deposited dose under different atmospheric concentrations of diesel exhaust particulate; application to aerosols with size distributions different from diesel exhaust particulate; use in the extrapolation of animal studies to humans; and identification of subpopulations that receive greater doses because of anatomical or ventilatory differences.

OBJECTIVES OF THE STUDY

The primary goal of this project was to develop and apply a mathematical model to describe the deposition and distribution of inhaled diesel exhaust particulate in the respiratory tract of humans and laboratory animals. The specific objectives, as described in the original proposal and in the final report, were to:

1. Analyze the physical characteristics of diesel exhaust particulate from automobile emissions on the basis of published experimental data;
2. Study the dynamics of diesel particulate in a model airway system adopted from published respiratory airway models;
3. Determine the role of diffusion, interception, impaction, and sedimentation in the deposition pattern of inhaled diesel exhaust particulate in the model airway systems;
4. Calculate from the model the regional deposition pattern and the deposition doses of diesel exhaust particulate in healthy human adults at resting breathing conditions;
5. Calculate the effect of different ventilation patterns on the regional deposition pattern and deposition dose;
6. Calculate the deposition pattern from airway models from infancy to adulthood in humans;
7. Calculate particle deposition doses in different laboratory animals, including rats, hamsters, and guinea pigs;
8. Extensively compare differences in species, including man, in regional airway deposition and tissue dose; and
9. Validate the model against measured deposition of diesel exhaust particulate in published animal experimental studies.

TECHNICAL EVALUATION

RESULTS AND INTERPRETATION

For their project, Drs. Yu and Xu made theoretical calculations of lung deposition so that airborne diesel exhaust particulate concentrations could be correlated with the amount and distribution of particulate material deposited in the lungs during inhalation. Factors considered to influence particle deposition included mean particle size*, degree of polydispersity*, ventilatory pattern, age, species differences, and body weight. The investigators considered a wide range of values, which approximated real-life conditions, for each factor. In addition, Drs. Yu and Xu developed a comprehensive lung growth model for humans from infancy to adulthood. They addressed and obtained results relevant to all of the specific objectives by valid and appropriate methods.

The results of the authors' calculations produced a number of interesting predictions. These include:

1. A three-fold decrease in mean particle size (0.3 to 0.1μm) only slightly increases deposition in the alveolar region (from 10 to 13%); however, a three- fold increase in the geometric standard deviation (σ_g)* around the mean particle diameter (at 0.2μm) increases alveolar deposition markedly (from 6 to 11%).
2. Nose versus mouth breathing increases head deposition ten-fold, but does little to "protect" the alveolar region where deposition is only slightly reduced.
3. A three-fold increase in minute ventilation* (from 10 to 30 liters) at low respiratory frequencies* (14 breaths per minute) nearly doubles the deposition efficiency*, thus resulting in an overall six-fold increase in the rate of particle deposition.
4. The deposition per unit tissue area in the unciliated airways is two-fold higher in children (two to eight years old) than in adults.
5. In laboratory animals, the deposition rate per unit unciliated tissue area is three to four times greater than in human adults.

*for an explanation of these terms, see page 25

Dr. Yu's study was entirely computational in nature. There is little experimental data to support some of the assumptions that were made to calculate regional deposition, or to verify the results presented. The lack of experimental verification does not adversely reflect on the quality of the investigation; it suggests that the model should be extensively tested against existing experimental results in animals and in man, and that further experimental work is needed to confirm the conclusions presented in the report. In addition, the mathematical and computational soundness of the formulae and calculations, upon which the input data and the model are based, should be affirmed.

More specifically, five considerations can be identified as limitations to the study:

1. In previous studies, the authors appear to have extensively reviewed data on lung architecture in the literature, but in this report, they do not fully justify the selection of the models that they used in the current study.
2. The model developed is based on a number of assumptions, some of which have little supporting experimental data, leaving some unresolved questions regarding the validity of the calculations based on these assumptions. These questions relate to: (a) upper airway deposition equations used to calculate nasal and oral deposition; (b) evaluation of head deposition efficiency in the laboratory animals; (c) geometric relationship of upper airways as a function of age; and (d) differences in size distribution and degree of dispersity between diesel exhaust particulate and other particles that have been used in human studies on head deposition efficiency.
3. The investigators found — not unexpectedly — that the deposition of submicron particles is governed primarily by diffusion. In view of the importance of diffusion, the equation used to describe the deposition efficiency of submicron particles might be reconsidered, even though it has long been in use.
4. The authors' discussion could be clearer and more complete with regard to: (a) the degree to which the model reflects reality; (b) the sensitivity of the results in relation to the nature of the assumptions made; and (c) the margins of error contained in the calculations.
5. The authors could state more clearly that the overall thrust of their report is on submicron particles of low density, which are deposited primarily by diffusion. Different results may be obtained with particles of different mean mass aerodynamic diameter, geometric configuration, or density.

These limitations, however, do not detract from interest in the project and its potential importance for the prediction of regional dose in the respiratory tract during exposure to ambient diesel exhaust particulate. The model appears to accurately reflect what is known in the literature, corresponds quite well with the animal data to which it has been compared, and is sensitive to structural and physiologic changes that occur with age and ventilation pattern.

NEW INSIGHTS

Mathematical modeling provides a valuable aid in understanding the operation of complex systems. The distribution of deposited material in lungs is an example of a phenomenon difficult to predict by intuition alone. Dr. Yu's model is particularly useful because it reflects variations in deposition dose to pulmonary tissues and appears to allow extrapolation across species. Potentially, the greatest impact of the project's results will occur when the model is further tested, and is considered in the context of a broader range of issues relevant to the regulatory questions involving diesel exhaust particulate.

CONCLUSIONS

The goal of the ideal exposure-dose model would be to predict the time course of particle concentrations within various body tissues as they relate to the concentration and character of inhaled aerosol. It is important to remember that the determining factors in such an ideal model include not only deposition distribution, but also clearance times and pathways of redistribution among cells and within tissues. Thus, Dr. Yu's model addresses only one component of site-specific retention, that due to initial deposition. Nevertheless, Dr. Yu's work represents one of the best efforts in mathematical modeling in respiratory biology; his model takes into account multiple factors that affect deposition, and thus comes closer to simulating realistic circumstances. Additional modeling research is needed to identify adequately the relevant issues in the translocation and clearance of deposited particles.

The project has clearly fulfilled the goals of both the HEI and the investigators. The work was well done, and is clearly described and well written. Major efforts should be made to further investigate the accuracy of the predictions from this mathematical model. Should the model's predictions prove to be valid, future research involving diesel exhaust particulate can be framed in the context of the expected lung burden predicted by the Yu model. The ability of this model to predict deposition dose from any given ambient exposure level would have a significant bearing on risk assessment, and would provide a tool for quantifying dose to target tissue from expected ambient or special condition exposure levels. Furthermore, the model could help identify health risks to susceptible persons on the basis of individual factors that govern regional dose in the respiratory tract. Potentially, the model could greatly improve the quantitative predictive power in the risk assessment process for diesel exhaust particulate, and perhaps it could provide an example for modeling approaches to the risk assessment of other mobile source airborne particles.

EXPLANATION OF SOME OF THE TECHNICAL TERMS USED IN THIS REPORT†

Deposition efficiency: Fraction of inhaled aerosol that deposits onto respiratory surfaces

Mass median aerodynamic diameter: The diameter of a unit-density sphere that settles at the same rate as an aerosol particle whose size is at the median of the particle size distribution

Mean particle size: Average diameter

Minute ventilation: The volume of air inhaled in one minute

Polydispersity: The degree of variation in particle size. Contrast with "monodisperse," which applies to an aerosol in which all the particles have the same size

Respiratory frequency: The number of breaths in one minute

σ_g: Geometric standard deviation around the mean particle diameter

†For a more complete discussion of these terms see Hinds, 1982

REFERENCES

Hinds WC, 1982. Aerosol technology: Properties, behavior, and measurement of airborne particles. New York: John Wiley and Sons.

Ishinishi N, Koizumi A, McClellan RO, Stober W (eds), 1986. Carcinogenic and Mutagenic Effects of Diesel Engine Exhaust. Developments in Toxicology and Environmental Science Series, Volume 13. Elsevier Science Publishers, Amsterdam, The Netherlands.

Schlesinger R, 1987. Biological disposition of airborne particles: Basic principles and application to vehicle emissions. In: Watson AY, Bates RR, Kennedy D (eds). Air Pollution, The Automobile, and Public Health: Research Opportunities for Quantifying Risk. Washington, D.C.: National Academy of Sciences Press (in press).

Valberg PA, 1985. Determination of retained lung dose. In: Witschi HP and Brain JD, (eds). Toxicology of Inhaled Materials. Heidelberg, West Germany: Springer-Verlag, pp. 57- 91.

ABOUT THE AUTHORS

C.P. Yu is Professor and former Chairman of the Department of Mechanical Aerospace Engineering at the State University of New York at Buffalo. He received his Ph.D. from Purdue University in 1964. In 1972, Dr. Yu spent a sabbatical leave at the University of Essex, England, and worked with Dr. C.N. Davies on aerosol deposition in human airways. Dr. Yu's primary research interests include the development of theoretical descriptions of aerosol deposition and the application of deposition models to various anatomical situations.

G.B. Xu received his Ph.D. from the State University of New York at Buffalo in June, 1986. He is currently a Senior Research Engineer at the Institute for Technology Development, Jackson, Mississippi, working on computer modeling of environmental protection problems.

FOR FURTHER INFORMATION CONTACT:

The HEALTH EFFECTS INSTITUTE
215 First Street
Cambridge, MA 02142
(617) 491-2926

HEALTH EFFECTS INSTITUTE
215 First Street • Cambridge, MA 02142
(617) 491-2926

RESEARCH REPORT No. 10: July, 1987